Aus dem Bereich Theoretische Medizin und Biowissenschaften
der Medizinischen Fakultät der Universität des Saarlandes,
Homburg/Saar

Multimodal attention in a simulated driving environment - Novel approaches to the quantification of attention based on brain activity

Dissertation zur Erlangung des Grades eines
Doktors der Theoretischen Medizin
an der Medizinischen Fakultät
der Universität des Saarlandes
2021

vorgelegt von:
Ing. Ernesto Gonzalez Trejo, M. Sc.
geboren am 17. März 1986 in Puebla, Mexiko.

Dekan: Prof. Dr. med. Michael D. Menger

Referent: Prof. Dr. rer. nat. Dr. rer. med. habil Daniel J. Strauss

Dedicated to my family

Tag der Promotion:	03. November 2021
Dekan:	Univ. -Prof. Dr. med. Michael D. Menger
Berichterstatter:	Prof. Dr. Dr. Daniel J. Strauß
	Prof. Dr. Tobias Hartmann

Abstract

The concept of attention is an established focus of study in neurosciences. The quantification of attention during driving can help identify situations in which the driver is not completely aware of the situation.

This work deals with the implementation of a setup to simulate a driving environment that enables audiovisual tasks to be embedded into the driving task while acquiring biosignals such as electroencephalography. The main goal of this dissertation was to find a correlation between attention and brain activity as seen on the electroencephalographic activity while driving. By using the principle of phase-amplitude coupling in electroencephalographic signals, it was hypothesized that Theta-Gamma phase-amplitude coupling might correlate to multimodal attention and thus might be eligible as a biomarker of attention in tasks such as driving. Surface electroencephalography was measured simultaneously in drivers and copilots while participating in simulated driving scenarios with varying multimodal attentional demands. The phase-amplitude coupling between Theta-band phase and Gamma-band amplitude from the electroencephalograpic signal was obtained and evaluated. Results showed significant phase-amplitude coupling differences between drivers and copilots in areas related to multimodal attention (prefrontal cortex, frontal eye fields, primary motor cortex, and visual cortex). The results were confirmed by behavioral data acquired during the test (detection task). We conclude that phase-amplitude coupling does function as a biomarker for attentional demand by detecting cortical areas being activated through specific multimodal (in this case, driving) tasks.

Additionally, the data acquired in the main work of this thesis was used to test an auditory stimulus reconstruction algorithm previously tested by our work group. The stimulus reconstruction allowed to obtain post-hoc additional information regarding attentional effort during driving (success of the stimulus reconstruction was significantly correlated to auditory effort) and serves as a compliment to the main results.

This dissertation thus offers an insight on attentional systems in multimodal situations and the neurophysiological systems underlying attention. It develops methods to measure attention in a driving environment, both as seen using phase-amplitude coupling and by being able to single out auditory effort by reconstructing the auditory stimuli. Finally, these methods can be translated to other activities since they are both based on non-invasive electroencephalography.

Zusammenfassung

Das Konzept der Aufmerksamkeit ist seit langem ein Schwerpunkt der neurowissenschaftlichen Forschung. Die Quantifizierung der Aufmerksamkeit während des Fahrens kann dabei helfen, Situationen zu identifizieren, in denen die Konzentration des Fahrers nicht ausreichend seien könnte.

Diese Arbeit befasst sich mit der Implementierung und Validierung eines Setups zur Simulation einer Fahrumgebung, die es ermöglicht, audiovisuelle Aufgaben in die Fahraufgabe einzubetten und gleichzeitig Biosignale wie Elektroenzephalographie zu erfassen. Das Hauptziel dieser Dissertation ist es, eine Korrelation zwischen Aufmerksamkeit und Gehirnaktivität zu finden, wie sie im Enzephalographie während der Fahrt zu sehen ist. Unter Verwendung des Prinzips der Phase-Amplitude-Kupplung (Phase-Amplitude Coupling) in elektroenzephalographischen Signalen wurde die Hypothese aufgestellt, dass die Theta-Gamma Phase-Amplitude-Kupplung mit multimodaler Aufmerksamkeit korreliert ist und daher als Biomarker für Aufmerksamkeit bei Aufgaben wie Fahren verwendet werden könntet. Oberfläche-Elektroenzephalographie wurde bei Fahrer und Beifahrer gleichzeitig gemessen, während beide an simulierten Fahrszenarien mit unterschiedlichen multimodalen Aufmerksamkeitsanforderungen teilgenommen haben. Die Phase-Amplitude-Kupplung zwischen der Theta-Band-Phase und der Gamma-Band-Amplitude aus dem elektroenzephalographischen Signal wurde gemessen und analysiert. Die Ergebnisse zeigten signifikante Phase-Amplitude-Kupplungsunterschiede zwischen Fahrer und Beifahrer in kortikalen Bereichen im Zusammenhang mit multimodaler Aufmerksamkeit (präfrontaler Kortex, frontale Augenfelder, primärer motorischer Kortex und visueller Kortex). Die Ergebnisse wurden durch Verhaltensdaten (während des Tests erfasster auditorischen Detektionstest) bestätigt. Wir schlieβen daraus, dass die Phase-Amplitude-Kupplung als Biomarker für den Aufmerksamkeitsbedarf fungieren könnte, indem es kortikale Bereiche erkennt, die durch bestimmte multimodale (in diesem Fall Fahr-) Aufgaben aktiviert werden.

Die für diese Arbeit aufgenommene elektroenzephalographische Daten wurden zusätzlich verwendet, um die Rekonstruktion des auditorischen Stimulus zu testen. Dafür würde ein Verfahren verwendet, die von unserer Arbeitsgruppe vor kurzem veröffentlich wurde. Die Ergebnisse haben zusätzliche Information bezüglich Aufmerksamkeitsbedürfnisse während des Fahrens geliefert und dienen, die Kernaussage dieser Arbeit zu unterstützen.

Diese Dissertation bietet somit einen Einblick in Aufmerksamkeitssysteme in multimodalen Situationen und in die zugrunde liegenden neurophysiologischen Systeme. Methoden wurden entwickelt, um Aufmerksamkeit zu quantifizieren, sowohl während der eigentlichen Aufgabe (wie aus den Phase-Amplitude-Kupplungsergebnissen hervorgeht) als auch durch die Rekonstruktion der ursprünglich verwendeten Stimuli. Die Post-Hoc Bearbeitung der Daten (Stimulusrekonstruktion) zeigt, dass diese Methode auch in unterschiedliche Situationen umgesetzt werden können.

Abbreviations

ADHD	attention deficit/hyperactivity disorder
Ag/AgCl	silver/silver chloride
ANOVA	analysis of variance
BSF	between-subjects factor (ANOVA)
DLPFC	dorsolateral prefrontal cortex
EEG	electroencephalography
EOG	electrooculography
ERP	event-related potential
FEF	frontal eye field
FIR	finite impulse response (filter)
fMRI	functional magnetic resonance imaging
fNIRS	functional near infrared spectroscopy
GSR	galvanic skin response
IC	independent component
ICA	independent component analysis
KL	Kullback-Leibler distance
MEG	magnetoencephalography
MI	modulation index
PAC	phase-amplitude coupling
PFC	prefrontal cortex
PMC	primary motor cortex
PVC	primary visual cortex
R1, R2	round 1, round 2 (time of measurement)
ROI	region of interest
SPL	sound pressure level
STG	superior temporal gyrus
WSF	within-subjects factor (ANOVA)

Contents

1 Introduction **1**

1.1 Attention 1

1.1.1 Visual Attention 2

1.1.2 Auditory Attention 4

1.1.3 Multimodal Attention 5

1.1.4 Attention in a Driving Situation 6

1.2 Quantification of Attention and Effort in a Driving Situation 7

1.2.1 Assessment of Brain Activity and Attention Using Frequency-Specific Components of EEG 8

1.3 Contribution of Thesis to Research Field 10

2 Materials and Methods **11**

2.1 EEG Phase/Amplitude Coupling in a Driving Situation 11

2.1.1 Motivation 11

2.1.2 Participants 11

2.1.3 Driving Simulator 12

2.1.4 Auditory Task and Stimuli 14

2.1.5 Task Scenarios 15

2.1.6 Psychophysiological Measurements 16

2.1.6.1 Data Acquisition 16

2.1.7 Subject Preparation 17

2.1.8 Data Processing 19

2.1.8.1 Electrooculography and Pupilometry 19

2.1.8.2 Galvanic Skin Response and Pulse Oximetry 20

2.1.8.3 EEG - Signal Conditioning 20

2.1.8.4 EEG - Phase-Amplitude Coupling 20

2.1.8.5 EEG - Band Power Analysis 26

2.1.9 Design of Analysis Tools 26

2.1.9.1 Mapping the 128-Channel EEG to a Plot 27

2.1.9.2 Plot - Raw Matrix 27

2.1.9.3 Plot - EEGLAB Topographical Map 27

2.1.9.4 Plot - 3D EEGLAB Topographical Map 28

2.1.10 Hypotheses / Expected Outcomes 33
2.1.10.1 Primary Hypotheses 33
2.1.10.2 Secondary Hypotheses 33
2.2 Additional Research Work 34
2.2.1 Participants 34
2.2.2 EEG Data Processing 34
2.2.3 Hypotheses / Expected Outcomes 37
2.2.3.1 Primary Hypotheses 37
2.2.3.2 Secondary Hypothesis 37
2.3 Statistical Analysis 37
2.3.1 Phase-Amplitude Coupling 37
2.3.2 Stimulus Reconstruction 38

3 Results **39**
3.1 EEG Phase/Amplitude Coupling in a Driving Situation 39
3.1.1 Behavioral Data (Detection Task) 39
3.1.2 Phase-Amplitude Coupling 39
3.1.3 Statistical Analysis - PAC 44
3.1.4 EEG Band Power 46
3.2 Additional Research Work 51
3.2.1 Stimulus reconstruction accuracy 51
3.2.2 Statistical analysis - stimulus reconstruction 51

4 Discussion **54**
4.1 Main work 54
4.1.1 Behavioral Task 54
4.1.2 Phase-Amplitude Coupling 54
4.1.2.1 High Gamma Band Activity in Surface EEG 55
4.1.2.2 Drivers Compared to Copilots 55
4.1.2.3 Band Power Analysis 56
4.2 Summary of PAC Results 56
4.2.1 PAC - Future Work 58
4.3 Additional Research Work 59
4.3.1 Stimulus Reconstruction Accuracy 59
4.3.2 Contribution to the Main Work 59

5 Conclusions **61**

Bibliography **63**

Publications by the author **72**

Acknowledgements **74**

1 Introduction

1.1 Attention

The concept of attention can be roughly summarized as the process in which the brain reacts to an external stimulus based on a given hierarchy (stimulus relevance), allocating cognitive resources to identify and respond to a particular stimulus while ignoring other, non-important information sources. How this hierarchy or relevance for a given stimulus is built, depends on several factors.
Here, we will categorize attentional processes into two: Top down and bottom up. Top down attention (also referred as endogenous, executive attention) refers to a response initiated by cortical structures and a certain expectation to the stimulus, while bottom-up attention (exogenous) refers to a raw stimulus, from which its physical attributes generate an instantaneous response, and is also referred as stimulus-driven attention (Katzuki and Constantinidis, 2014; Connor et al., 2004). Both types of attention do not work separately, but instead they influence each other (Wolfe, 2010) and it has been argued that creation of of priority maps for a given scene are mediated by both at the same time (Katsuki and Constantinidis, 2012). As noted in the review from Corbetta and Shulman (2002), functional magnetic resonance imaging (fMRI) and electroencephalographic (EEG) studies have pinpointed top-down networks in parietal and posterior frontal cortices, while bottom-up networks involve temporo-parietal junctions and ventral frontal areas from the right hemisphere.

The attention directed to stimulus defined by bottom-up (i.e. exogenous) factors depends mostly on contrast (i.e. how the target stimuli differs from it surroundings, e.g., color, pitch) (Duncan and Humphreys, 1989). Incoming information is arranged in a global map (the "bottom" stage); afterwards, information is processed according to features and each stimulus is then represented by a corresponding feature map (e.g. color). The last step (the "up" stage) involves the contrast (or "saliency") of a given stimulus in this map; attention is then redirected to the element on the map presenting the most salient activation (Koch and Ullman, 1985). On the other hand, attention to top-down stimuli, the context (e.g. field of view, auditory scene) needs to be thoroughly analysed (Wolfe and Horowitz, 2004) and is associated with an increase on firing rates of neuron groups coding specific features of the perceived scene (Desimone and Duncan, 1995), effectively biasing the response to non-relevant features and allowing selective attention. Moreover, top-down attention is considered to be a voluntarily-initiated process (for an in-depth analysis of the mechanisms underlying both systems, and both local and global neuro-modulatory circuits, see Avery et al. (2014), who used a 2-cortical column model to study the mechanisms at work at single-neuron level, based on the Izhikevich neuron model).

1.1.1 Visual Attention

In bottom-up attention, visual competition starts when salient stimuli activate receptive fields as early as the V1 area of the visual cortex; this saliency continues to be represented on its way up, it is however not enough to direct attention to a stimuli. Instead, attention has to be oriented by using information coming from cortical areas responsible not only for the central visual field, but the peripheral field as well. Moreover, saliency maps require feedback from cortical areas such as the frontal eye fields/prefrontal cortex (Katsuki and Constantidinis, 2014).

Regarding top-down attention, visual stimuli have to compete against all sensory information arriving at the brain at the same time. However, this process is started voluntarily and is thought to have its origin on higher cortical areas such as the prefrontal cortex and the posterior parietal cortex (PFC having a direct influence on a behavioral response) (Katsuki and Constantidinis, 2014). As mentioned before, the bias of non-relevant stimuli allows for selective attention and this in turn allows the modulation of visually evoked responses (Buschman and Kastner, 2015). However, the process in which a visual stimuli is assigned top priority starts previously, in what has been called "preparatory attention" (Battistoni et al., 2017). Preparatory attention (also referred as attentional set, attentional template or search image) involves creating an internal representation of a scene (e.g. before crossing a street, we expect to see traffic lights, cars and pedestrians without having a-priori information about a specific street crossing) and might involve a pre-activation of the visual cortex, even in the absence of visual input. As shown by Posner et al. (1980) and Kasper et al. (2015), having information regarding the location of a stimulus before it is presented (preparatory attention is therefore present) speeds up response times and facilitates search tasks. Information regarding the content, as opposed to (or together with) the location of the stimulus has also been shown to enhance responses (Stein and Peelen, 2015). While both spatial-based and content-based attention regulate visual evoked responses, they modulate such responses in different ways (Ling et al., 2009). The concept of preparatory attention thus describes everyday situations better than visually-evoked potentials (e.g. having information at hand regarding the scene before us, such as a driving situation and what we expect from it, compared to a flashing screen where a target has to be found). Of relevance to this work is the fact that through preparatory attention, the possible distractors in a scene are potentially pre-filtered (Battistoni et al., 2017), enhancing the attentional response to relevant stimuli (in this case stimuli related to the task of driving).

A concept that overlaps with selective attention and is of special relevance to the work at hand is "visual search". In this case, the visual input must be processed, but any information regarding the scene at hand is absent. For example, driving in an unknown city and trying to find traffic signs, street names, or information or cues to arrive at an unknown address. The information needed (i.e. the target) might not have enough contrast against all incoming information, therefore making recognition of salient features more difficult and requiring increased attentional resources. This requires for the person to form a mental representation of the target with the information at hand, and to compare it in real time to the input received through visual (or multimodal) stimuli. As suggested by Eimer (2015), we can recognize four phases of this process: Preparation, guidance, selection and recognition; each phase involves different brain processes.

The first phase, preparation, involves the creation of search templates in visual working memory, which itself requires prefrontal cortical areas to regulate the access to working memory and maintain memory representations of the desired target in an active status until feedback is received.

The guidance phase gathers target-relevant features once the results of the visual search are available (e.g. a visual scene is presented); possible targets are therefore limited to the information provided by the scene itself and modulated by attentional templates (generated in the preparation phase). This feature-based step allows the identification of potential targets within the visual field, which are then represented through priority or salience maps.

Once potential targets are selected in the guidance phase, the selection phase allows to allocate focal attention to possible correct targets; it specifically refers to a particular stimulus (target) successfully driving neural activity towards a location (spatial focal processing) and inhibiting or lowering the relevance of the remaining scene elements.

Finally, recognition happens once these correct targets reach visual working memory and are successfully compared to the templates created previously (it is not enough to choose an object or target; the features of the selected objects have to be integrated). If an ac-

tive representation of the selected object is found within working memory, the object is then recognized. This requires therefore a sustained focus on the selected target and a sustained representation of the search template in working memory.
The visual search process, and more specifically the last step involving attentional resources (recognition) can be measured (EEG, ECoG, fMRI, MEG). The prefrontal cortex was previously thought of being responsible for storing information in working memory, however, as reviewed by (Lara and Wallis, 2015) working memory is achieved by several cortical regions, including both the prefrontal cortex and posterior sensory cortices.

1.1.2 Auditory Attention

Analog to visual attention, auditory attention may also be described in terms of top-down and bottom-up processing. A study by Bidet-Caulet et al. (2015) suggests that bottom-up resource allocation has a stronger influence on attention than top-down processes, when dealing with distracting stimuli.

The first step in the process of directing attention to a specific target, is the decomposition of the overlapping sounds arriving at the same time into the ear. This is called auditory scene analysis (Bregman, 1990). This process starts already within the auditory pathway, without requiring attentional resources (Pressnitzer et al., 2008) (frequency separation and directionality, for example). The problem of mixed sources, in which cognitive resources are needed to extract and identify a single source as a target was coined "cocktail party problem" by E. C. Cherry Cherry (1953). The effect of attention can be measured using event-related potentials (ERP) and paradigms such as oddball or mismatch negativity paradigms. The components of the ERPs are selectively sensitive to attention (e.g. components N1 and P2 from late ERPs appear regardless of the attention of the subject; however, attentional tasks affect the amplitude and latency of these components and complex tasks elicit additional waves such as the P3 wave). The function and/or contribution of the auditory pathway to the process of perception (or at least the activation of subcortical structures as a reaction to a stimulus) can be also measured using early auditory ERPs (Luck, 2005). There are a myriad of studies involving variations of the basic auditory evoked potentials and attention paradigms (a PUBMED search for publications including "auditory evoked potentials" in their title returns over 90 publications as of January 2021; several thousands if the terms are extended to the publication's full text).

The direct relation between working memory load and auditory attention was studied by Sabri et al. (2014). A relation between the N1 component of the auditory ERPs and activity in medial prefrontal cortex and superior temporal gyrus (STG) was observed. In parallel, interactions between memory load and irrelevant speech activated STG and frontoparietal areas, suggesting these areas may process auditory distractions and the N1 component might be an indicator of such processing. Working memory performance did not change in the presence of irrelevant speech.

Another factor facilitating attention (or even enabling it in the first place) is sensory gating / inhibition of non-relevant sensory information. This gating, or inhibition of non-relevant input can be seen in pre- and post-attentional evoked responses in healthy subjects (Rentzsch et al., 2008) and deficiencies might work as indicators for neurophysiological conditions such as schizophrenia (Boutros et al., 2004) and attention-deficit hyperactivity disorder (ADHD) (Micoulaud-Franchi et al., 2015).

1.1.3 Multimodal Attention

The efficiency of solving a multimodal attentional task increases when multisensory information is congruent (Dhamala et al., 2007) and decreases when one of the modalities presents conflicting/non-congruent information (Mayer et al., 2009). Both modality specific mechanisms and top-down cognitive processes have to work in tandem to obtain congruent information. Competition between auditory and visual stimuli requires top-down attention. This has been suggested to rely on Theta (4-8 Hz) oscillations in frontal cortex, which might act as an organizing system between feedback loops across the cortex (Cavanagh and Frank, 2014) and have a role in top-down control (Cohen and Donner, 2013). Wang et al. (2016) observed that both visual and auditory attention modulate Theta band activity.

A very interesting interaction between auditory and visual responses to a stimulus is presented by Escera et al. (2000), in which novel (i.e. bottom-up salient) stimuli elicited prolonged reaction times to visual targets; however, the auditory stimulation in this case preceded the visual target in a constant, predictive fashion on every occasion, allowing for preparatory attention to be formed (as the auditory information is task-related). In another study, where the novel auditory stimulus contained no information regarding the task (i.e. did not allow to predict it), the reaction time was not affected; only when the auditory stimulation was target-related, an impairment in the visual response was seen

(Wetzel et al., 2013).

Interaction between visual and tactile information and attention shifts was studied via ERPs by Katus et al. (2017). Using visual and tactile stimuli (and cued by auditory stimulation), they have shown that visual information remains in working memory even when no longer required due to relevant stimuli still being present in another modality (e.g. tactile). Contrary to this, the tactile representations in working memory disappeared when they became irrelevant; both showing that top-down processes have an influence on working memory representations of stimuli (i.e. relevance of the stimuli is important) but also suggesting that the representation of visual elements in working memory is more complex than tactile representation.

Studies with patients suffering of mild traumatic brain injury have allowed to pinpoint certain areas that allow selective attention; in Mayer et al. (2012) bilateral dorsolateral prefrontal cortex and bilateral visual streams indicated attention-modulating activity (i.e. top-down cognitive control) only in healthy subjects. Moreover, task-induced deactivation was absent from patients.

1.1.4 Attention in a Driving Situation

Driving is a complex cognitive task, involving audiovisual cues, mechanical coordination, decision making and information retention, among others elements, which have to be processed simultaneously (Schweizer et al., 2013). Attention to the driving task is therefore of utmost importance; even a slight distraction can lead to a dangerous situation. Current technological advances such as navigation systems, hands-free systems, smart cockpits and mobile phone interfaces offer support to driving tasks, but act also as a distraction (Tijerina et al., 2000; Horrey and Wickens, 2004; Owens et al., 2011; McGehee, 2014). Moreover, they usually overlap natural distractions such as passengers, weather and/or traffic conditions, or those caused by fatigue effects (Young and Regan, 2007; Sagaspe et al., 2008; Lin et al., 2016).

Recent efforts to characterize or predict driving behavior include the work of Yan et al. Yan et al. (2019), who analysed EEG data (using event related potentials (ERPs) where the event was turning in an intersection on the road) together with a personality factor questionnaire (splitting subjects into four personality trait groups). They found a correlation between the personality traits and the activity seen in the EEG (e.g., the unreasoning group had higher car collision rate and intensive driving action, and a stronger activation in motor and sensorimotor areas) suggesting predicting and/or preventing dangerous driving behaviours might be possible.

Even with automated vehicles, attention is still required, as the current technology is at a state in which safety cannot be guaranteed at all times and in certain situations, the vehicle requires the input of the driver. Solis-Marcos et al. Solis-Marcos et al. (2017) studied attention allocation in partially automated driving using auditory ERPs (oddball task) and found that the automation level affected the attention of the driver, as seen in the auditory P3 component, even after short periods of driving. The reduction could be caused either by an underload effect (low demand task due to automation), and as time increases, due to fatigue (regardless of automation).

1.2 Quantification of Attention and Effort in a Driving Situation

The current challenge in research lies in the assessment of perceptual and cognitive workload in a driving situation. Functional magnetic resonance imaging (fMRI) (Calhoun et al., 2001; Calhoun and Pearlson, 2012; Just et al., 2008; Kan et al., 2013; Schweizer et al., 2013; Chung et al., 2014) and magnetoencephalography (MEG)(Bowyer et al., 2009; Fort et al., 2010; Sakihara et al., 2014) have located key areas involved in driving tasks such as the primary motor cortex, visual cortex, prefrontal cortex, superior frontal gyrus and parietal lobes. These studies have also shown a decrease in driving performance by tasks such as language comprehension (Just et al., 2008) and conversation (Bowyer et al., 2009), suggesting a different process between external (driving task) and internal (cognitive task) attentional effort; however, they are mostly limited to a virtual environment. For real-life driving situations, portable solutions have been developed; these include, for example, electroencephalography (EEG) (Jap et al., 2009; Lin et al., 2011, 2005; Lei and Roetting, 2011; Li and Chung, 2015; Wascher et al., 2016) and functional near infrared spectroscopy (fNIRS) (Yoshino et al., 2013; Oka et al., 2015; Nosrati et al., 2016). These non-invasive methods allow for an easier setup and measurement of brain activity both in virtual and in real driving situations; although the information obtained is limited by the constraints of measuring neuronal activity at the scalp, both techniques provide a way to confirm existing studies and allow for more flexible situations and novel study designs, which may even combine both EEG and fNIRS (Ahn et al., 2016).

1.2.1 Assessment of Brain Activity and Attention Using Frequency-Specific Components of EEG

While the amplitude of the EEG signals in time domain is used for analysis (as described in the previous sections regarding auditory and visual attention by using ERPs), the frequency components both in oscillatory (i.e. continuous) and evoked (i.e. studying the immediate response in a small window in time post-stimulus) have shown to offer more information about brain activity than the time domain alone, both regarding band power, frequency contribution and onset/offset of certain frequency bands for certain tasks.

Not only are EEG features described based on frequency bands (Alpha, Beta, Gamma, Delta and Theta), but simple experiments as the Berger effect (Kirschfeld, 2005) allow to demonstrate that certain frequency bands are dominant above others in certain situations. A common indicator of neural activity in situations such as driving has been the quantification of the contributions from the different EEG frequency bands (Engel et al., 2001). For example, Gamma activity has been shown to correlate with sensory processing, attentional and memory tasks (Tallon-Baudry et al., 1997; Gruber et al., 1999; Herrmann et al., 2004; Jensen et al., 2007), while Theta has been related with error processing, working memory and information encoding (Klimesch, 1999; Cohen, 2011; Gärtner et al., 2014; Arrighi et al., 2016).

Moreover, ERPs are not necessarily evoked by changes in amplitude of EEG frequency bands (Sauseng et al., 2007). This may be explained by the nature of neural activity, in which the synchronization (firing in a certain frequency) of a neuron population and their phase differences affects the resulting brain activity (in this case the summation of their action potentials, perceived as amplitude). Nevertheless, both techniques can be used together to acquire additional information as shown by van den Berg et al. (2016), where decreased Alpha-band oscillations were related to preparatory attention and N1 amplitudes were related to post-stimulus responses and learning effects.

The effects of Alpha, Beta and Theta frequency bands in goal-directed and involuntary visual attention were shown by Harris et al. (2017). The goal was to capture oscillatory activity elicited by task-irrelevant cues. They found that Theta oscillations lateralized according to the position of the stimulus, suggesting feature-based stimulus enhancement; Alpha oscillations lateralized only after target-matching cues, suggesting involvement in allocation of spatial attention, even in involuntary conditions. Previously, attended and unattended states on firing patterns and synchronization (e.g. Gamma frequency power as indicator of desynchronization) of neuronal populations were studied by Harris and Thiele (2012); they found that suppression of spontaneous activity (e.g. appearance of synchronized activity) could be regarded as a form of attention, in which synchronized firing acts as a suppressor of interfering, non-relevant stimuli.

Combining EEG with fMRI has also allowed to pinpoint generators of frequency-based activity; Green et al. (2017) studied visual spatial attention and found that occipital Gamma-band EEG correlated to activity in visual cortical regions contralateral to stimuli and ipsilateral Alpha-band activity, which acted as attention-related inhibitor. Summarized, this points Gamma waves as an enhancer and Alpha waves as a suppressor of attention. The activity of Alpha band as a suppressor has also been observed in auditory tasks and stream segregation (Melnik et al., 2017; van Diepen and Mazaheri, 2017; Weise et al., 2016); an increase in Alpha band power related to acoustic detail in an auditory distractor also suggest the role of Alpha as a suppressor of unwanted information (Wöstmann et al., 2017).

Neuronal oscillations are the base of cognitive activity (Buzsáki and Draguhn, 2013; Fries, 2005), but the interaction between different frequency bands is still being studied (Uhlhaas et al., 2009). Cross-frequency coupling has received a lot of attention in recent years, by proving to be a neural marker of cognitive processing in humans (Jensen and Colgin, 2007; Cohen, 2008; Jirsa and Müller, 2013). Especially Theta-Gamma, phase-amplitude coupling (PAC) (Tort et al., 2010; Canolty et al., 2006), which has been related to sensory integration, working memory (Lisman, 2005; Dimitriadis et al., 2015) and visual perception (Bruns and Eckhorn, 2004; Demiralp et al., 2007), which are essential to driving tasks (Lei and Roetting, 2011).

1.3 Contribution of Thesis to Research Field

This thesis deals with the development of state-of-the-art techniques to assess attention and cognitive workload during driving situations, both for drivers and copilots, using high-resolution EEG systems and processing information in both the time and phase domains of the acquired signals. In the main work of the dissertation, the phase-amplitude coupling (PAC) framework established by Tort et al. (2010) was used in order to analyse EEG acquired during driving. The primary outcome was to analyze the feasibility of PAC as an indicator of attentional effort. If a feature can be identified within the EEG that allows to differentiate both active (driving) and passive (copilot) or high-attentional and low-attentional situations, the benefits for the design of user interfaces within vehicles could be significant (e.g. to assess if the driver is paying attention to the road ahead). Moreover, it might also contribute to the current literature regarding multimodal attention and how the attentional resources are assigned in the brain during tasks. To the knowledge of the author, there is currently no technique that allows to distinguish a high attentional workload during driving in an objective manner, and no technique that does so by measuring drivers and copilots at the same time.

As an additional research work, the data used for PAC was then used post-hoc to reconstruct the auditory stimuli used during the measurements; as shown by our workgroup previously (Schäfer et al., 2018), a correlation between auditory attention and successful stimulus reconstruction is possible. The stimulus reconstruction results thus complement the observations made with the PAC methods.

The tools developed to process the high-definition EEG (to obtain PAC) were also assessed by colleagues in the research group (SNN-Unit) and validated by being used for EEG measurements not related to driving; it is the hope of the author that not only the final results of this dissertation are of use to the research field, but the methods and tools developed to acquire, process and analyse the resulting data might as well be of further use.

2 Materials and Methods

2.1 EEG Phase/Amplitude Coupling in a Driving Situation

2.1.1 Motivation

The main work for this dissertation resulted in a setup for a driving simulator, in which the multimodal (audiovisual) tasks overlapping the driving task could be customized at will. The attention required to successfully completed the tasks (while driving) was studied using electroencephalography (EEG) by combining both amplitude and phase information from the EEG, using the Phase-Amplitude Coupling method established by (Tort et al., 2010). The goal was to be able to observe different levels of cognitive effort / attentional demand elicited by multimodal tasks (driving situation) and measured objectively using EEG. Moreover, this setup allows for real-time measurements and an additional test subject can be added (copilot), the hypothesis being that the copilot could serve as a control condition between active and passive driving.

2.1.2 Participants

Twenty-two healthy subjects (3 female), ages between 20 and 29 years (M = 24.4 $\pm$ 2.7) took part in the study. All subjects were right-handed, German native speakers and were required to have a valid driver's license (mean driving experience 6.8 $\pm$ 2.3 years); subjects were recruited from the social environment of the authors. The subjects had no hearing/visual impairments (contact lenses were allowed if they were required according to their driver's license). Before each measurement, the subjects were informed about the objectives and methodology of the measurement and gave their written consent. No history of neurophysiological diseases/impairments was present on any of the subjects. The measurements were performed at the MINDSCAN Laboratory from the Systems Neuroscience and Neurotechnology Unit in Saarbruecken, Germany. The design of the study was written following ethic guidelines and the declaration of Helsinki; each participant was given the choice to abandon the measurement at any given time.

2.1.3 Driving Simulator

The indoor driving simulator consists of a real commercial vehicle cockpit (Audi A3, 2013) with an interface connected to a personal computer; the interface transfers information from the steering wheel and pedals to the simulation software (simulator interface and software engine from Simutech GmbH, Bremen, Germany). The software displays the virtual environment along three monitors. Driving in the simulation requires the same actions as real-life driving with a manual, 5-gear gearbox transmission; all pedals (gas, brakes and clutch) are functional. Speedometer and revolution-counter (RPM) are also connected to the software and display the speed/RPM in real time. The software simulation renders a small city, rural roads and/or highways, or a combination of them, according to the designed task. Pedestrians, traffic and randomized events such as pedestrian cross-walks, wild animals or construction sites appear during driving and can be turned on or off. Road navigation systems are also integrated (NAVI) and guide the subjects from beginning to end of the task through audiovisual cues (arrows displayed between speedometer and tachometer and auditory playback of spoken directions). Weather conditions (day/night, rain, snow, fog) can also be modified according to the task at hand.

The auditory output from the simulation software was re-routed to a separate personal computer, which also was used for additional auditory stimuli/task playback. A 24-loudspeaker array (JBL Control 1 Pro Loudspeakers, JBL, California, USA.) was mounted around the cockpit allowing a directional control of auditory stimuli / distractions during driving. Each loudspeaker was controlled independently through audio-processing software (PreSonus Audio Electronics, Louisiana, U.S.A.). Loudspeakers were grouped in three circular arrays, with a 45° angular resolution at floor (8 speakers, 40 cm high), ear (8 speakers, 115 cm) and over-the-head (8 speakers, 190 cm) heights.

Both the audio coming from the driving simulator software as well as the audio used for the auditory tasks were first converted to analog using a digital/analog interface (RME Digital/Analog Interface M-32 DA, RME Audio AG, Haimhausen, Germany). The loudspeakers were driven using 3 8-channel power amplifiers (Apart PA8250, Apart Audio NV, Antwerp, Belgium). Additionally, two sub-woofer systems were embedded under the cockpit, in order to elicit low-frequency vibration akin to the one present while driving. The subwoofers were driven using two additional power amplifiers (the t.amp S-100 mk2, Thomann GmbH, Burgebrach, Germany; BKA 1000 N, The Guitammer Company, Ohio, USA.). Fig. 2.1 shows the layout of the driving simulator.

All audio used was fine-tuned and calibrated (intensity and position) to allow for a realistic spatial sound localization from the seat of the driver. This included varying amplitude of combined speakers and cross-mixing two or more speakers in order to enhance the directionality of the sound (e.g., sounds perceived as coming from the back seat or cockpit seat).

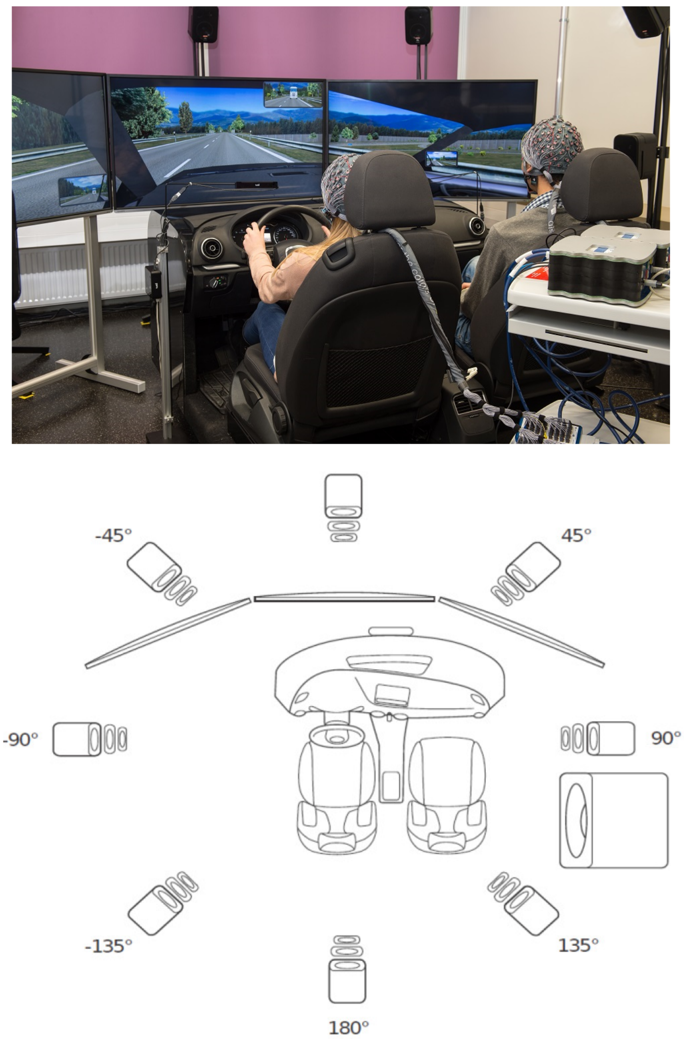

Figure 2.1: Layout of driving simulator: (top) A real automobile cockpit is used, together with software rendering a virtual environment on three monitors in front of the driver and a multi-directional speaker array, which provides auditory feedback, tasks and distractions according to needs. (Bottom) Speaker array: 24 speakers are arranged around the cockpit and allow for controllable spatial localization of sounds. Several speakers can be linked together in order to simulate spatial localization more accurately (e.g., back seat or cockpit seat), or can be used independently. The subwoofer system under the cockpit is not shown.

The driving task within all modalities of the study was to drive correctly (following traffic laws) around the selected environment, following the directions of the NAVI system. If a subject was detected not following traffic laws (e.g., speeding, running under red lights), the measurement was stopped and restarted after reminding the subject of the correct driving behaviour expected. According to the selected modality, the driving conditions vary (more/less traffic, bad weather) to increase or decrease the difficulty of the driving task. Additionally, eye tracking hardware (Tobii Pro X2 60, Tobii AB, Sweden) was used to monitor the gaze of the subjects in real time and ensure that they were looking at the screens during the measurement; both driver and copilot were reminded before each measurement to keep their eyes on the road during driving tasks.

2.1.4 Auditory Task and Stimuli

The main auditory stimuli used for the tasks was a radio broadcast (in German) while driving. According to the modality (scenario) of the study at hand, the subjects were asked to detect a specific word within the broadcast ("und") and press a button, or do nothing and keep driving with the broadcast still playing. The word was chosen due to the number of occurrences in the selected radio broadcasts and due to being one of the most used words in German language (Ruoff, 1981).

In order to increase the difficulty of the task, background noise was added. The main component of the background noise was the so-called "Fastl Noise" (Fastl, 1987), which simulates spectral and temporal features of human speech. This noise was implemented in the same loudspeakers as the radio broadcast. Additional auditory distractors were implemented coming from different directions: Recordings of babies crying and kids arguing were played from the loudspeakers simulating the back seats, while mobile-phone ringtones were played from the side loudspeakers to appear coming from the seat next to the driver. The sounds were temporally distributed along the task, care was taken to ensure that none of the distractors overlapped the target words thus rendering them imperceptible.

All sounds were calibrated in order to attain safe hearing amplitude levels and strictly kept under 80 dB SPL. The maximum amplitude recorded (driving at maximum speed, with all auditory stimuli being played at the same time) was 72.3 dB SPL. The Fastl noise was set at 66,5 dB SPL in order to obtain a signal-to-noise ratio (SNR) between radio broadcast and Fastl around -1.5. The radio broadcast contained conversations from several participants and the amplitude varied between 64.8 and 65.6 dB SPL (playback amplitude set to 65 dB SPL), therefore the actual SNR measured varied between -0.9 and -1.7. This was deemed as adequate for the given tasks. The additional noises (kids, baby, mobile phone) were all played at 64 dB SPL.

The beginning of each task, the task word and the button press produced non-audible trigger signals, which were sent to the data acquisition system through a trigger box (g.Trigbox, g.Tec, Austria) for post-hoc signal processing.

2.1.5 Task Scenarios

Three main tasks were designed ("A", "B" and "C"), each 4 minutes in length, which involved different degrees of auditory and visual or non-auditory attentional effort in driving. Driving in task "A" was done in a highway without traffic, without speed limit and with clear weather and no randomized traffic events. Driving in tasks "B" and "C" started in a rural road and crossed through an urban environment; for both B and C the weather was set as rain with fog and a sight distance ahead of 40 meters, forcing enhanced driving effort. The tasks can be summarized as follows:

- Task "A": Driving effort: low; auditory effort: high. Driving in the highway without traffic and with a clear weather, while solving the auditory task (pressing a button when "und" is heard) in the presence of auditory distractors.
- Task "B": Driving effort: high; auditory effort: low. Driving in a mixed environment with bad weather conditions; no auditory distractors, radio broadcast playing but button should NOT be pressed.
- Task "C": Driving and auditory effort: high. Driving in a mixed environment with bad weather conditions, while solving the auditory task (pressing a button when "und" is heard) in the presence of auditory distractors.

Besides the main tasks, two training stages and an initial baseline measurement were performed:

- Baseline: No tasks, driving simulator off, 80 seconds.
- Driving Training: Free driving in an urban environment, 2 minutes.

- Auditory training: Broadcast was presented with occurrences of the target word and button should be pressed, driving simulator off, 80 seconds.

After the main tasks were performed, tasks A, B and C were repeated in a randomized order, as a re-test to enhance the robustness of the results (referred from now on as 2A, 2B and 2C). The scenarios and their distribution along the measurement are shown in Figure 2.2.

Two subjects were measured at the same time, for each measurement (driver and copilot). Once the measurement was finished, the current driver and the copilot switched places and the measurement was restarted. Due to the subjects not being naive any more to the measurement, the second measurement was classified differently from the first: subjects from the first measurement were classified as "round 1" (Driver and Copilot R1), and subjects from the second measurement (non-naive) were classified as "round 2" (Driver and Copilot R2). An example setting for the audio playback software is shown in Figure 2.3.

2.1.6 Psychophysiological Measurements

2.1.6.1 Data Acquisition

Electroencephalogram (EEG) was acquired using a high-resolution EEG system (g.Tec, Austria) with 128 active electrodes, at a sampling rate of 512 Hz. Impedances for the active electrodes were kept under 50 kΩ. No online filtering was used and all electrodes were referenced to CPz and re-referenced to the average reference post-measurement. The average reference method is regarded as the best approximation to a "neutral" reference when using EEG systems with 30 or more channels, see (Dien, 1998; Ferree, 2000; Hagemann et al., 2001).

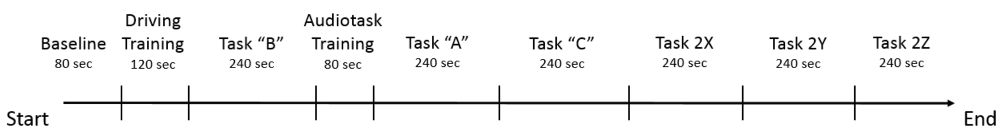

Figure 2.2: Measurement plan. A baseline, two training stages and three different tasks are planned. The three tasks (A, B, C) are then repeated in a randomized order (here shown as X, Y and Z) for re-test purposes.

Figure 2.3: Studio 1 software overview. The software allows to split tasks, distractions and triggers into different audio tracks and control both the volume and the directionality of each one separately. Each track can be assigned to one or several of the 24 speakers in the system.

Additionally, two passive Ag/AgCl electrodes were placed around the left eye in order to acquire electrooculography (EOG) and detect blinking; a pulse oximeter (g.PULSEsensor, g.Tec, Austria) and galvanic skin response (GSR) electodes (g.GSResponse, g.Tec, Austria) was fixed to the left (right) hand of the driver (copilot)

All biosignals (EEG, EOG, pulse, GSR), together with the trigger signals from the auditory stimuli and button, and eye position tracking were acquired through a biosignal amplifier (g.HiAmp, g.Tec, Austria), all with a sampling rate of 512 Hz and controlled through a SIMULINK interface (The Mathworks, Massachusetts, USA), see Figure 2.4. Two workstations were used, one for the driver and one for the copilot, with identical data acquisition setup. The output file was processed using MATLAB R2013a (The Mathworks, Massachusetts, USA). An example of the various output signals obtained is shown in Figure 2.5

2.1.7 Subject Preparation

After the subjects read and signed the consent forms, the Ag/AgCl electrodes for EOG were placed. Once fixed, the subjects were asked to sit in the driving simulator and the EEG cap was placed on their heads. The subjects received a button for solving the task; in the case of the driver, the button was fixed to the side of the index finger of the right hand. This position allowed the driver to press the button with the thumb without leaving the steering wheel. The pulse and GSR sensors were placed in the left hand of the driver and in a way that they allowed for a natural position of the hand on the steering wheel.

Once all sensors were in place, the subjects were informed of the course of the measurement. They were not informed of the auditory task until the auditory training took place. Between each task, there was a small pause (approximately 1 minute) where the subjects were asked if the measurement may continue. If so, the operator informed them of the upcoming task and checked that all sensors were still working correctly (e.g., impedances from the EEG and EOG electrodes still within acceptable ranges).

At the end of the measurement, the subjects answered a small questionnaire regarding their perception of the difficulty of the tasks, their performance, the level of distrac-

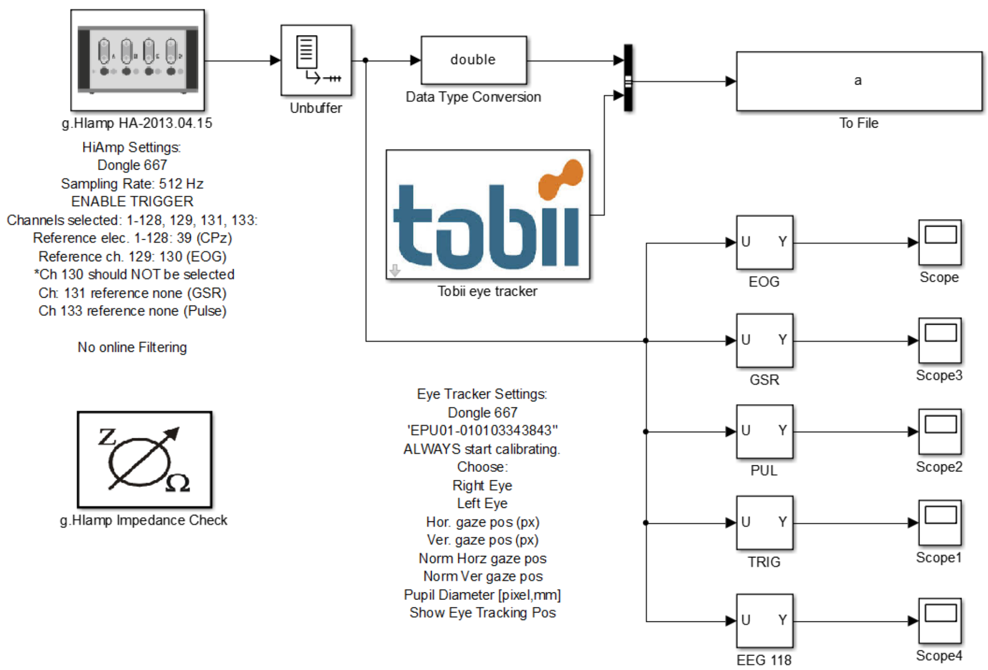

Figure 2.4: SIMULINK block program. The high-resolution amplifier (HiAmp, top left) allows to set the sample rate and choose how many electrodes will be acquired, together with the reference. EOG, pulse and GSR are acquired by the amplifier as well. Real-time filtering can be applied (not used; only post-filtering was applied outside SIMULINK). Both the EEG and the eye tracker data are acquired simultaneously and saved into a file ("a" in the figure). At the same time, a series of scopes allow to monitor the measurement in real time. This setup was run in parallel, one in a computer acquiring the EEG of the driver and eye tracker data and a separate computer for the EEG of the copilot and eye tracker data.

tion attained through the audio system and the quality of the simulation overall. As a safety measurement, subjects were not allowed to drive their vehicle 30 minutes post-measurement.

2.1.8 Data Processing

2.1.8.1 Electrooculography and Pupilometry

The EOG data was processed using MATLAB functions. The raw signal was filtered with a FIR bandpass filter (2-20 Hz, order 1500, Hamming window). The data was used for eye-artefact (blinking) recognition, but not used for additional analysis. The pupilometry information was also recorded directly from hardware; using the SIMULINK interface, it was used during the measurement to control the gaze position and ensure that both driver and copilot were looking at the screens at all times. The data was not analysed for this work but was saved for future analysis.

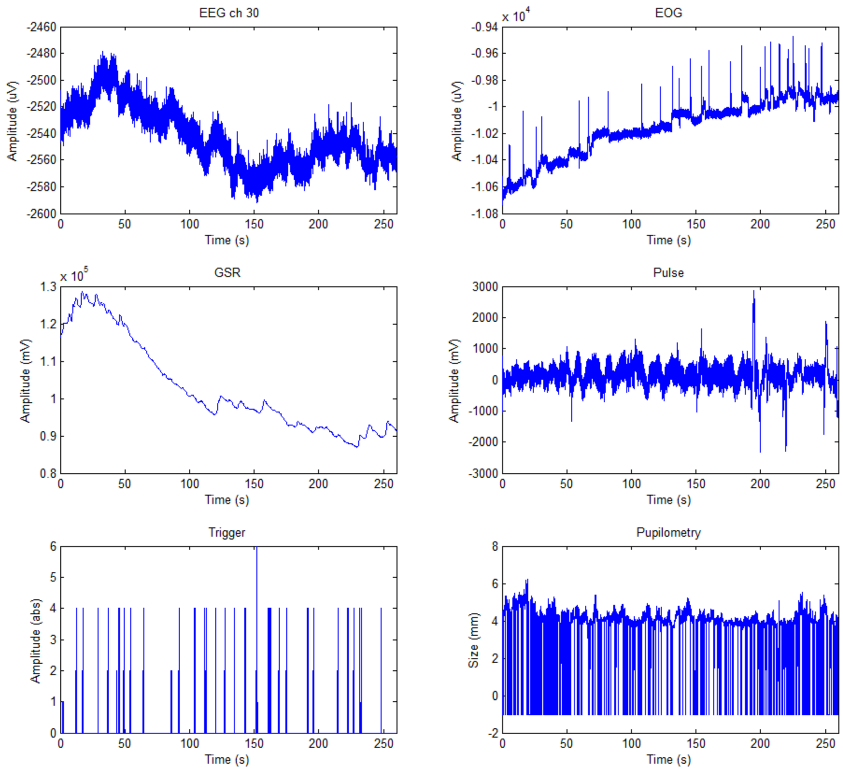

Figure 2.5: Examples of signals acquired (unfiltered): (top left) EEG; (top right) EOG; (middle left) GSR; (middle right), pulse; (lower left) task triggers; (lower right) pupilometry.

2.1.8.2 Galvanic Skin Response and Pulse Oximetry

GSR and Pulse were also obtained in raw form and stored for post-analysis; they are not analysed in the scope of this work but were stored and may present additional information for future work.

2.1.8.3 EEG - Signal Conditioning

The first step in the processing of the acquired (raw) EEG signals was the removal of the blinking artefacts by using independent component analysis (ICA)-based blind-source separation. This was implemented using the EEGLAB Toolbox (SCCN, San Diego, USA.) in MATLAB and the FastICA (Hyvärinen and Oja, 2000) algorithm. ICA was performed for the 128 EEG channels and the independent components (ICs) were individually analysed to search for recognizable blinking artefact patterns. Once found, these ICs were removed from the original signal. Care was taken in order to only remove the ICs corresponding to eye artefacts, even if in some cases the eye artefacts were not completely removed. This compromise was chosen in order to keep as much signal integrity while removing as much artefacts as possible. The output signal post-ICA was manually compared to the original raw signal and to the EOG raw signal, in order to confirm that the artefacts removed were indeed caused by blinking, as shown in Figure 2.6. Examples of artefact-ridden ICs are shown in Figure 2.7.

After removing the eye artefacts, the EEG data was re-referenced to the average reference.

2.1.8.4 EEG - Phase-Amplitude Coupling

The phase-amplitude coupling analysis was done following the framework established by (Tort et al., 2010); what follows is a brief description of the procedure.

In order to analyse the phase-amplitude coupling, the EEG signal is split into 3 frequency bands: theta (4-8 Hz), low gamma (30-50 Hz) and high gamma (50-80 Hz), using a FIR filter with a Hanning window in MATLAB. It has been argued that the useful spectrum of EEG that can be measured through scalp EEG is limited to 80 Hz (Canolty et al., 2006; Jensen and Colgin, 2007). Based on this assumption, we limited our analysis accordingly. We split the gamma (30-80) frequencies into two sub-frequencies, from now on denoted as low (30-50 Hz) and high (50-80 Hz) gamma, and studied both conditions simultaneously. The mean of the filtered signals is subtracted afterwards and the phase information is extracted.

The phase information of a signal $s(t)$ (in this case, our EEG signal) can be obtained from its complex analytic form:

$$\bar{s}(t) = s(t) + jH_{\mathrm{s}}(t)$$

In the time domain, the Hilbert transform of a function $s(t)$ is defined as the convolution between the $1/(\pi t)$ operator and the function $s(t)$. David Hilbert is credited with showing that the function $sin(\omega t)$ represents the Hilbert transform of $cos(\omega t)$ in the complex notation of harmonic wave forms derived by the Euler formula

$$e^{\mathrm{jz}} = cos(z) + jsin(z)$$

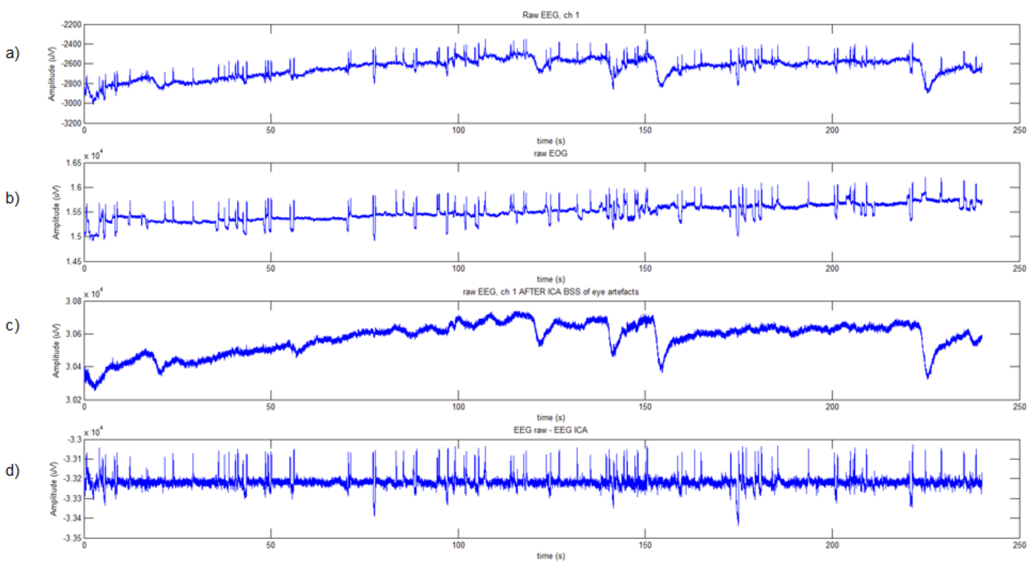

Figure 2.6: Removal of eye artifacts from EEG using ICA. The raw EEG (a) is contaminated with muscular artifacts from blinking, which can be seen on the acquired EOG (b). Using ICA and removing the components located close to the eyes (and manually inspected in order not to remove critical information), the resulting EEG signal mantains its morphology (c). In order to confirm that ICA worked correctly, the post-ICA EEG signal was substracted from the raw EEG signal. The remaining noise (d) corresponds to the blinks detected by the EOG, therefore confirming that blinking was removed by ICA.

(expressed as $cos(\omega t) + sin(\omega t)$ by Kennelly and Steinmetz).

This gives us in turn the phase shift operator $\pm\pi/2$, a basic property of the Hilbert transform. The relationship between a function $f(t)$ and its Hilbert transform is orthogonal and called the "strong analytic signal", with both amplitude and phase components, where the derivative of the phase component becomes the instantaneous frequency of the signal. The Fourier transform of the strong analytic signal produces a one sided spectrum in frequency domain (i.e. no negative frequencies are obtained).

We can then use the Hilbert transform to create an analytic signal from a real signal, which allows to obtain a vector with the instantaneous phase $\phi(t)$ and instantaneous amplitude $A(t)$ in the time domain. Therefore, we can write the strong analytic signal as follows:

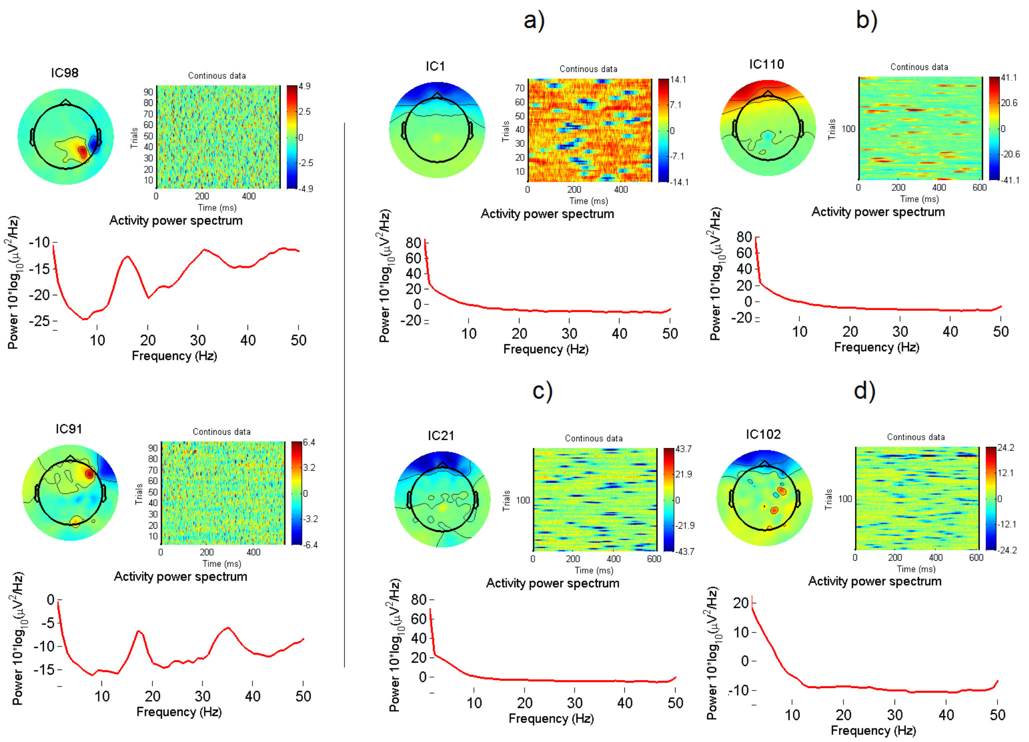

Figure 2.7: Independent components (ICs) manually chosen to illustrate EEG data (left column) and eye artifacts (marked a to d). The EEG data presents frequency spectrum peaks corresponding to alpha and beta/gamma activity, while the eye artifacts present a flat spectrum. Moreover, when stacking the EEG in sweeps (marked as "continuous data"), big traces are visible in a,b,c,d. Both the frequency spectrum and the traces in big data were used as a criteria to manually select the ICs to remove using ICA.

$$\bar{s}(t) = s(t) + jH_{\mathrm{s}}(t) = A(t)e^{i\phi(t)},$$

where

$$A(t) = \sqrt{s(t) + H_{\mathrm{s}}(t)}$$

and

$$\phi(t) = arctan(\tfrac{H_{\mathrm{s}}(t)}{s(t)})$$

For a thoroughly demonstration of the Hilbert transform see Johansson (1999).

The Hilbert transform is applied to both theta and gamma acquired signals; the phase is then extracted from the Hilbert transform of the theta-filtered signal and the amplitude envelope is extracted from the Hilbert transform of the gamma-filtered signal. This allows for a representation of the amplitude of the gamma oscillations at any given phase value of the theta oscillations.

The phase information is then split in 18 bins (each accounting for 20-degree changes) and the mean amplitude (acquired from the gamma oscillations) over each phase bin is calculated. Finally, the mean amplitude values for each bin are normalized; the normalized amplitude acts a discrete probability density function. For no phase-amplitude coupling, the amplitude distribution (P) over the phase bins would be uniform; therefore, a deviation from an uniform distribution denotes coupling. The deviation is calculated using an adapted Kullback-Leibler distance (KL) in order to obtain deviation values between 0 and 1. The KL distance is defined as

$$D_{KL}(P,Q) = \sum_{j=1}^{N} P(j)log\left[\frac{P(j)}{Q(j)}\right].$$

Moreover, the KL distance can be expressed in terms of the Shannon entropy H of a P distribution, as

$$D_{KL}(P,U) = log(N) - H(P),$$

where U is the uniform distribution. Here, *log(N)* corresponds to the maximal possible entropy value (uniform distribution). A modulation index (MI) is then calculated, by dividing the KL distance by *log(N)*

$$MI = \frac{D_{KL}(P, U)}{log(N)}.$$

For an uniform distribution of the amplitude over the phase values, the MI is 0; a value of 1 would correspond to a distribution centred on a specific bin (a Dirac distribution) representing a gamma oscillation that only occurs in a single phase bin of theta.

The MI presents very low values (as seen in (Tort et al., 2010), a "locked" theta-phase gamma-amplitude modulation would reach a MI value around 0.015 in ideal, simulated conditions). It is also important to note that the value is sensitive to the noise within and the length of the measurement (the measurement has to have at least more than one cycle of the phase information). The training tasks (baseline, driving and auditory training) are

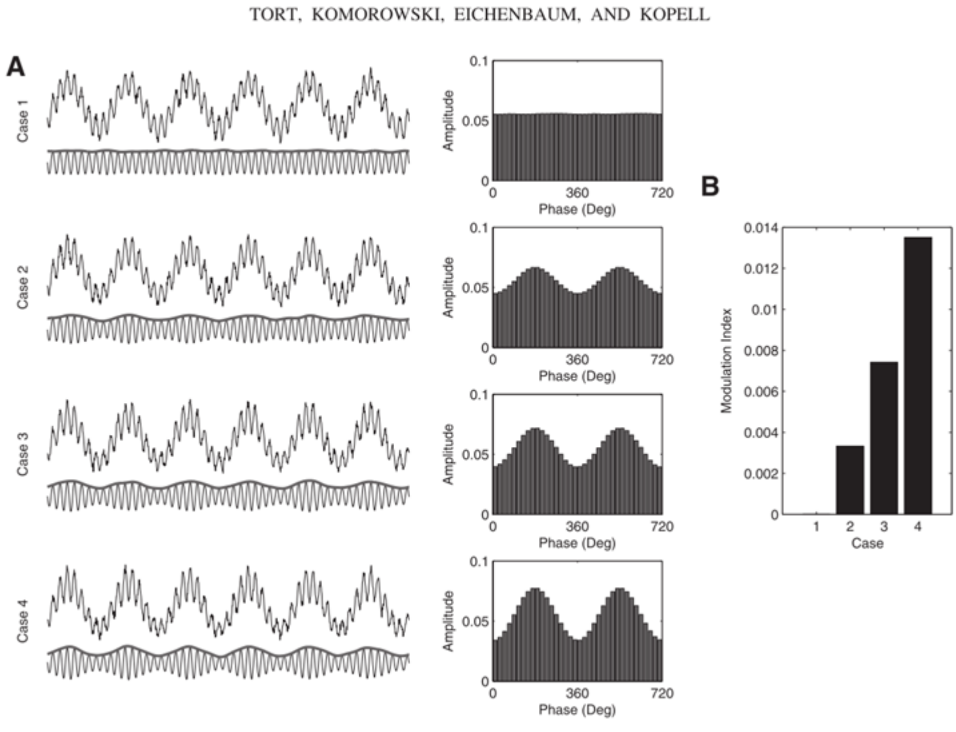

Figure 2.8: The phase-amplitude coupling (PAC) principle (Taken from Tort et al. 2010). Four cases are presented. In case 1, the theta signal has no effect in the gamma signal (envelope marked with a thick line), which equals a modulation index of zero. The more influence theta signal has on gamma (as seen in the phase) (A), the higher the modulation index obtained (B). The middle column (A, right) shows the phase-amplitude plots (each bar represents a phase bin).

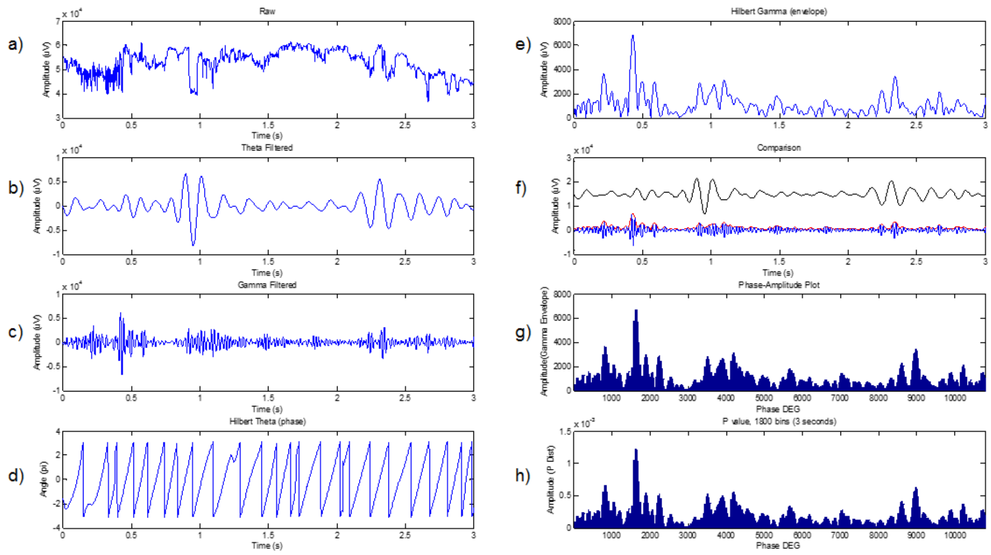

Figure 2.9: PAC implementation in MATLAB. a) Raw EEG signal. b) Theta-band EEG filtered signal. c) Gamma-band EEG filtered signal. d) Instantaneous phase obtained from the theta-filtered EEG signal (using Hilbert). e) Envelope obtained from the gamma-filtered EEG signal (using Hilbert). f) Comparing the theta filtered EEG signal (top, equals b), the gamma-filtered EEG signal (bottom, blue, equals c) and the gamma envelope (bottom, red, equals e). g) Phase-amplitude plot (theta bins against gamma envelope amplitude). h) normalized amplitude value (amplitude distribution value P) instead of gamma amplitude.

shorter (80 seconds) than the main tasks (240 seconds) and therefore present larger MI values (longer measurements present a smaller MI variation, allowing for a stabilization of the values). The scale in the figures presented in the results section was adjusted to reflect this.

The MI was calculated for each channel, for each task, for each subject separately. Once finished, the mean for each subject group was calculated, for each of the tasks (e.g., all drivers, drivers from first round separately, all copilots and so on). The MI values were then plotted over the scalp using EEGLAB-based scripts. If an electrode had a MI value 3 times bigger than the average value of all electrodes, it was considered a faulty electrode; its value was then assigned based on its nearest neighbours. Measurements with more than 10 faulty electrodes were not taken into account. For the final analysis, 18 of the original 22 subjects were considered, based on the quality of the measurement. Figure 2.8 resumes the PAC procedure (from (Tort et al., 2010)). Figure 2.9 shows an example of the steps implemented in MATLAB to obtain PAC from the EEG signals in the study.

2.1.8.5 EEG - Band Power Analysis

The individual power of specific EEG frequency bands is one of the most widely analysis used regarding functional tasks (e.g. see Klimesch (1999); Mai et al. (2016); Grummett et al. (2014); Gruber et al. (1999)). In order to compare the phase-amplitude coupling analysis to established methods, the band power was analysed as well, for drivers and copilots (from both stages) and for each task.
In order to calculate band power, the following frequency bands were defined: theta (4-8 Hz); alpha (8-13 Hz); beta (13-30 Hz), low gamma (30-50 Hz) and high gamma (50-80 Hz). The raw EEG signal from each channel was then filtered using a FIR bandpass filter (order 1500) with a Hann window. Two methods were tested to determine the band power: the first involved obtaining the power from the Fourier transform of the EEG signal for each task, for each electrode; the second method involved the use of the BANDPOWER function in MATLAB. The second method was chosen due to its faster implementation and the ability to process all the 128 EEG channels at once (as a matrix).

2.1.9 Design of Analysis Tools

Given the amount of data obtained from a single measurement (128 channels, 9 tasks, approx. 30-minute EEG recordings at 512 Hz sampling frequency, plus ICA components), new methods for the display and analysis had to be developed from scratch. Raw matrix, topographic head models in 2d, 3d and animations were developed for the analysis of the data. One objective when developing such tools was for them to be available for subsequent measurements and to be as flexible as possible, allowing their use for studies with similar EEG systems but different data processing requirements. This was validated during the study as the topographic mapping was constantly requested and used by pilot studies not related to the work presented here. All analysis tools were developed using MATLAB R2013a (The Mathworks, Massachusetts, USA), EEGLAB Toolbox (SCCN, San Diego, USA.) and either self-programmed functions or EEGLAB-based functions. In this section, each approach will be presented independently, in order to allow its reproduction.

2.1.9.1 Mapping the 128-Channel EEG to a Plot

The first obstacle to overcome was the correct mapping of the HiAmp system 128-channel EEG cap to MATLAB. Unfortunately there are no official templates available and the manufacturer failed to provide a solution. Therefore, two approaches were tried: Raw matrix and topographic (the latter based on EEGLAB).

2.1.9.2 Plot - Raw Matrix

First, each electrode was mapped to an element in an 11x18 element matrix in MATLAB (handled as an image). This provided a raw representation of the topography, but was very abstract in practice. Using the function IMRESIZE in MATLAB, the values were interpolated by a factor of 10 (Gaussian interpolation) in order to obtain a softer looking image. The results of this representation are shown in Fig 2.10.

2.1.9.3 Plot - EEGLAB Topographical Map

Since the matrix representation was deemed too abstract, a better approach was implemented. Based on the built functions of the EEGLAB Toolbox, a mapping of the 128-electrode EEG cap was adapted to the polar coordinates used by EEGLAB to create a location map within a head contour. The actual coordinates were calculated by hand based on the existing diagrams from the manufacturer of the EEG cap. This is implemented in a ".loc" file; the structure can be modified in any text editor and consist of 4 tab-separated columns: column 1 represents the electrode index (1 until 128); column 2 represents the angle (polar coordinates); column 3 represents the distance from origin (polar coordinates) and column 4 is the label of the electrode. By modifying this file, a location file can be created for virtually any electrode configuration.

Once the location file was available, a plotting function was written in MATLAB (based on EEGLAB topographic plotting). The function obtains the value for a single moment in time, for each electrode and maps them to a 2D circular surface. This surface is then adjusted to the head shape according to the polar coordinates of each electrode and labelled. Figure 2.11 shows the steps in this process. The scale of the head and the circular surface was adjusted in order to contain the information within the head shape; therefore certain electrodes were not accounted for (the most distal electrodes).

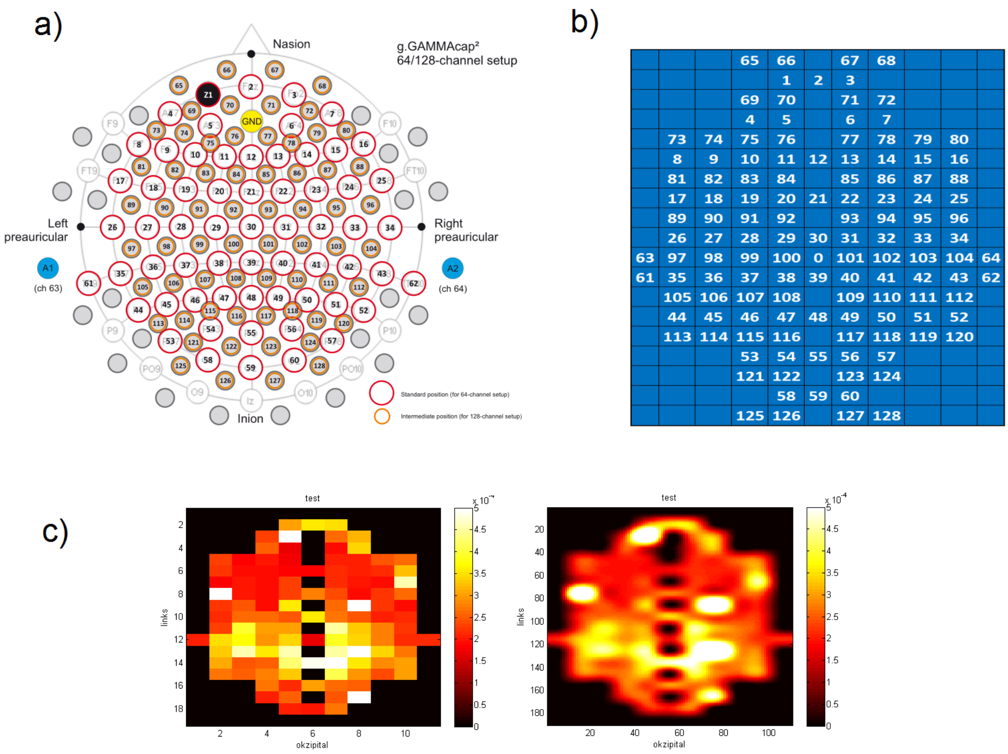

Figure 2.10: Mapping of the 128-channel high-resolution EEG system. a) The topographic map provided by the manufacturer. b) Each electrode was assigned to a position in a 19x11 matrix in MATLAB. c) The values acquired in each electrode is assigned to the corresponding element in the matrix; the matrix shows the value of all electrodes at the same time, for a single moment in time. d) The matrix is interpolated by a factor of 10 (Gaussian interpolation) in order to obtain a smoother image, which can be used to create animations.

Although this representation provides a better insight into the localization of EEG activity compared to the raw matrix, it can be enhanced in two ways: a 3d representation can be created as well, and a new dimension (time) can be added, by creating several "snapshots" or data points in time, and joining them into a "GIF" image. Both approaches were implemented; due to the limitations of a printed work, the GIF cannot be shown, but the code for their creation, together with the plotting code are available from the SNN-Unit workgroup.

2.1.9.4 Plot - 3D EEGLAB Topographical Map

Finally, an additional function based on the EEGLAB toolbox was implemented, in order to map the 2D surface created for the topographic map into a 3D surface. Al-

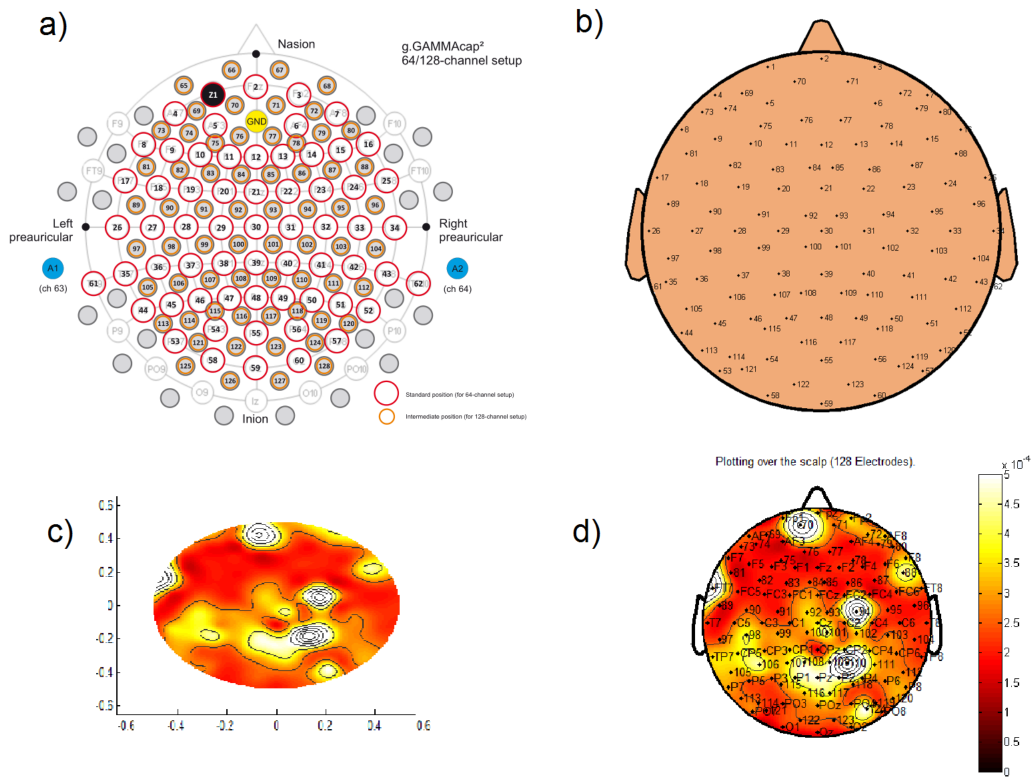

Figure 2.11: Custom-created 2D topographical maps. a) The topographic map provided by the manufacturer. b) A topographic map custom made using EEGLAB tools for plotting EEG data, corresponding to the electrode positions shown in the topographic map of the manufacturer. c) The EEG data of each electrode plotted in a 2D surface (EEGLAB script). d) The EEG data surface is adjusted to the custom topographic map and the electrode positions and numbers are added.

though EEGLAB provides a 3D object (mesh) in which the surface can be projected, it was decided to use an alternative 3d mesh, with better quality. The chosen mesh was sourced from "http://www.turbosquid.com/3d-models/male-head-obj/346686"; authored by "Mad Mouse Design" and is provided with a royalty-free license. The 3D head was imported to MATLAB and EEGLAB was used to create a spline file (Figure 2.12), which maps the electrode positions and the surface information to the surface of the head. The preliminary results are shown in Figure 2.13. Thanks to the customized functions used, specific colormaps can be created to improve the look of the results, or to streamline the design according to established standards (useful for publication). This flexibility is shown in Figure 2.14

Both the 2D as well as the 3D representations of the results were used; 3D results were

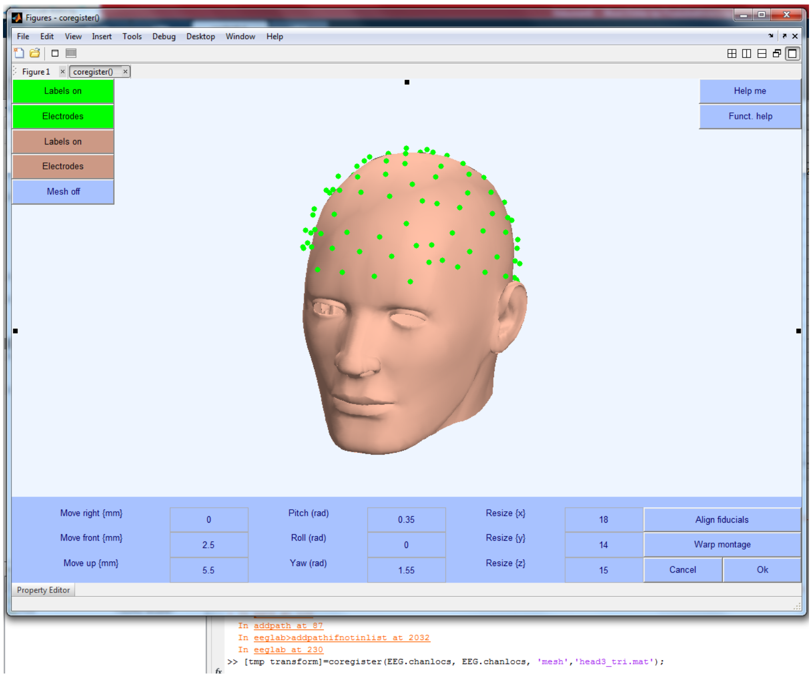

Figure 2.12: Using the electrode location file from EEGLAB and a 3D head model to coregister electrode locations in 3D. The 2D head has to be adjusted (resized and tilted) to fit the 3D model. The interface is also part of the EEGLAB toolbox.

used when a specific area was studied, while 2D was used to provide an overall view of cortical activity. The results presented in this work are based on the 2D view. Finally, a comparison of all the techniques implemented is shown in Figure 2.15, for the same time snapshot (data sample).

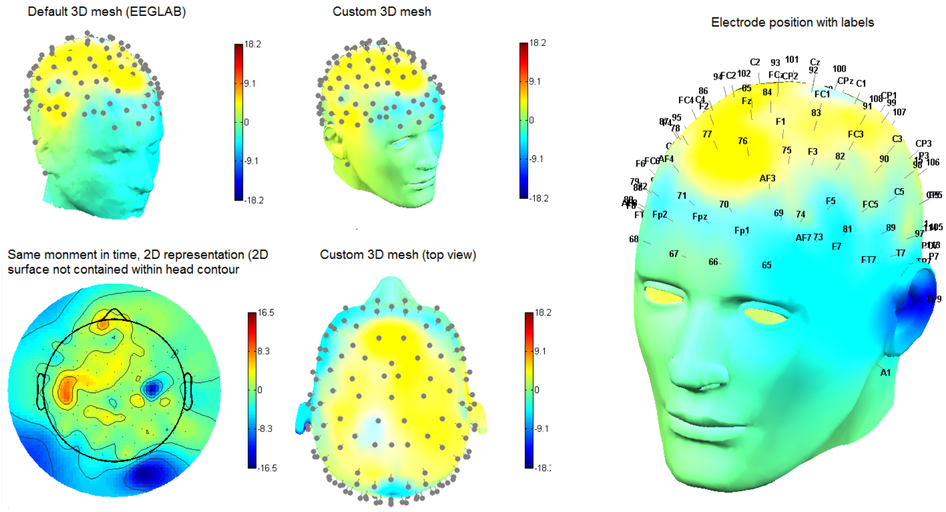

Figure 2.13: Comparing the default EEGLAB 3D head ("mesh") (top, left). The mesh was made using fMRI imaging. The custom 3D mesh is a generic 3D head that aims to represent any subject. The 2D surface created previously (bottom left) is mapped over the 3D head. The electrode positions are projected and labelled. This allows for a more realistic localization of brain activity than 2D maps.

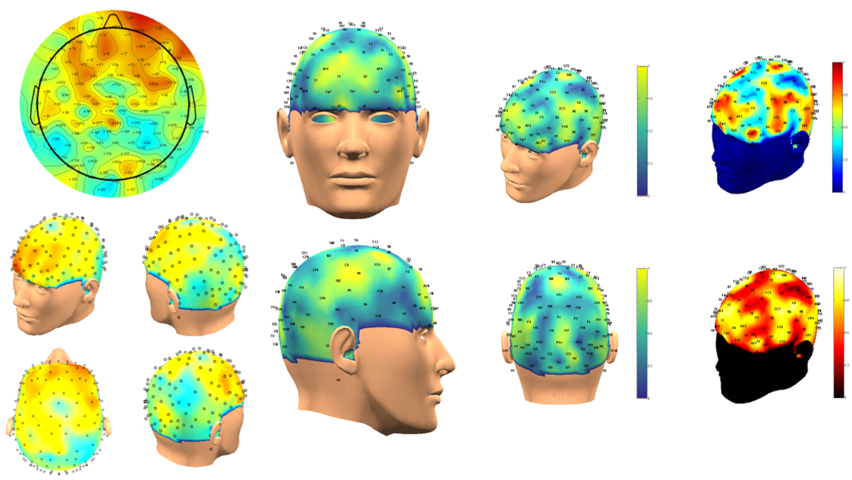

Figure 2.14: Once the maps are projected into the 3D head, the color maps can be modified to obtain a more realistic representation, or a more adequate color representation. Here, custom colormaps for MATLAB are shown ("jet", "parula" and "hot", modified to show a simulated skin color)

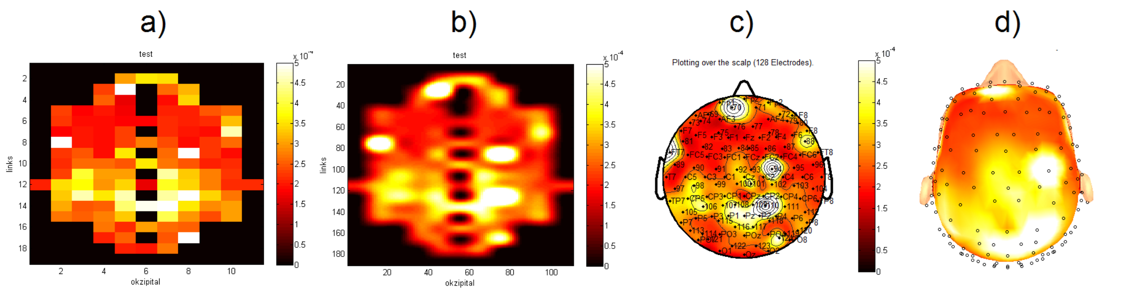

Figure 2.15: Plot comparison for a single time frame. a) Matrix representation of electrode values. b) Smooth (Gauss) interpolated matrix representation. c) Electrode information projected into a 2D topographic map using EEGLAB functions. d) 2D topographic map projected into a 3D head model using EEGLAB functions.

2.1.10 Hypotheses / Expected Outcomes

2.1.10.1 Primary Hypotheses

- Theta-phase / Gamma-amplitude coupling (PAC) might work as a biomarker of cortical activation related to cognitive effort while driving; a higher PAC in cortical regions of interest should be observable (e.g. prefrontal cortex, visual cortex, motor cortex, frontal eye fields, auditory cortex).
- Cognitive effort from drivers and copilots as seen in PAC should differ and show areas that are more/less active (e.g. motor areas in the driver not seen in the copilot, audiovisual areas in the copilot).

2.1.10.2 Secondary Hypotheses

- Relevant information from the high-Gamma domain (50-80 Hz) can be measured using surface-EEG only and therefore PAC can be measured using the high-Gamma domain as well.
- An increased PAC should be visible on the auditory cortex given the nature of the measurement (auditory detection task - auditory scene analysis).

2.2 Additional Research Work

Since a high volume of EEG data was generated to analyse the phase-amplitude coupling (PAC), the data was also used to validate the work published by the work group in (Schäfer et al., 2018), where EEG was used to reconstruct features of the auditory stimuli used such as attended/unattended states, by considering the brain/EEG a linear, time-invariant (LTI) system where the input (auditory stimulus) is mapped to an output (EEG) and then the system is solved backwards (EEG used to reconstruct the auditory stimulus) (Crosse et al., 2016).

Of special interest was to find out if the stimulus reconstruction could be used in such a demanding environment as the one constructed for this dissertation, instead of more controlled conditions as originally tested. Therefore, no changes or additional measurements were done and instead the same EEG data obtained for the PAC measurements were used as input for the auditory stimulus reconstruction task. We expected to see a higher stimulus reconstruction accuracy whenever the auditory distractors were lower and therefore the attention could be focused on the stimulus, thus allowing a more reliable reconstruction. This would in turn also validate the previous claim that the setup presented in this work is able to elicit different levels of attentional effort.

Finally, the results from PAC and stimulus reconstruction are compared and a suggestion on how to combine both algorithms to obtain as much information regarding the attentional demands during driving is presented (results currently on submission for publication).

2.2.1 Participants

The same participants and measurements as described in the PAC measurements were used; only the data processing differed, as follows.

2.2.2 EEG Data Processing

For the analysis, all EEG data was stored as an NxT matrix, where N denotes the number of EEG channels and T denotes the time points (recorded data points at 512 Hz, thus each T are data recorded each 0.00195 seconds). Unlike the PAC measurements, only 61 EEG channels were needed for the stimulus reconstruction algorithm (equally distributed across the scalp following the international 10-20 EEG placement system). Then, all channels were filtered using a zero phase-shift, finite impulse response (FIR) bandpass filter from 1 to 45 Hz. The filter was based on a Hamming window, with an order of 1000. The filtered EEG channels were then segmented into the different scenarios used in the PAC measurements described previously (baseline, trainings, tasks A, B, C, 2A, 2B and 2C), based on the trigger signal acquired. In order to ensure adequate data quality, each EEG channel was then transformed into the frequency domain using the fast Fourier transform (FFT) and its spectrogram analysed; peaks in Alpha activity were then detected (between 8-13 Hz). Only channels with detectable Alpha activity were used for the stimulus reconstruction. Moreover, only scenarios in which the subjects were confronted with the stimulus material (i.e. the tasks: A, B, C, 2A, 2B and 2C) were used, for both the driver and passenger situations. This resulted in 2x6 measurement blocks of about four minutes each and thus about 48 minutes of analysable data material per subject.

In order to prepare the EEG data for stimulus reconstruction, the data were then additionally filtered with a zero phase-shift FIR bandpass filter between 1 and 15 Hz (anti-aliasing filter). Afterwards, the data sets were downsampled from 512 Hz to 128 Hz. Finally, the first 3.5 minutes are taken from the four minutes long blocks and split into 30 seconds long sub-blocks. Thus, for each subject and each scenario seven 30-second EEG data blocks with 61 EEG channels each are generated, i.e., r(t,n), where t denotes samples in time and n denotes the EEG channels. In this format, the EEG data is ready as input for the stimulus reconstruction algorithm. The stimulus reconstruction algorithm requires the recorded neural activity as well as the physical characteristics of the acoustic stimulus as input. Accordingly, the audio files used for stimulation in the driving simulator for the main work of this thesis were also fed to the algorithm. The first step was to calculate the broadband envelope of each radio segment according to the equation

$$xa(t) = x(t) + ix \wedge (t) \tag{2.2.1}$$

where xa(t) represents the complex analytic signal resulting from the complex sum of the audio file's segment x(t)and its representation in Hilbert space x∧(t). The speech envelope is defined as the absolute value of xa(t), that is, e(t)=|xa(t)|. The envelope was sampled down from 44.1 kHz to 128 Hz following the application of an anti-aliasing filter. The final step was to separate the calculated envelopes into 30-second snippets so as to match them to their corresponding EEG segments.

The measurements analysed consist of a total of ten measuring sessions with two subjects each - once as a passenger and once as a driver, just as in the main work using PAC. Data is thus available for each participant, from six hearing situations (tasks A, B, C, 2A, 2B and 2C), i.e. there are 248 EEG data blocks r(t,n) for each hearing situation (124 as driver and 124 as passenger). Within a leave-one-out-cross-validation process, the optimal decoder g is determined from 237 of the 248 EEG blocks and the corresponding stimuli. With the help of this decoder, a reconstructed stimulus is calculated based on the 248th EEG data block that is still unseen by the algorithm. This results in 248 reconstructed stimuli. These are then compared with the actual stimuli using Pearson's Rho. This results in 248 correlation coefficients for each subject and for each listening situation. Only significant correlation coefficients were used for evaluation ($p<0.05$). Table 2.1 gives an overview of the generated output.

Table 2.1: Significant correlation coefficients used for evaluation (from 120 available)

		significant corr. coefficients
Round 1 (R1)	Task A Driver	75
	Task B Driver	77
	Task C Driver	63
	Task A Copilot	69
	Task B Copilot	85
	Task C Copilot	81
Round 2 (R2)	Task A Driver	73
	Task B Driver	69
	Task C Driver	66
	Task A Copilot	69
	Task B Copilot	80
	Task C Copilot	82

The final results are mean values calculated only from the significant correlation coefficients for the respective groups. The stimulus reconstruction accuracy measures the average correlation coefficient according to Pearson between actual stimulus and EEG-reconstructed stimulus for the respective group.

2.2.3 Hypotheses / Expected Outcomes

2.2.3.1 Primary Hypotheses

- The features of auditory stimuli (radio broadcast) can be reconstructed using the surface EEG (e.g. attended/unattended states)
- The stimulus reconstruction provides additional information regarding a subject's attentional state during a driving situation, which wasn't seen with the PAC algorithm.

2.2.3.2 Secondary Hypothesis

- The results show that the stimulus reconstruction algorithm as prepared by our work group can be used in data that was not acquired specifically to be analyzed with it.

2.3 Statistical Analysis

2.3.1 Phase-Amplitude Coupling

To assess if there was indeed a significant difference between drivers and copilots in general, a mixed-ANOVA test using the PAC of each single electrode as the dependent variable was used (between-subjects factor: driver/copilot; within-subjects-factor: tasks). The difference between drivers "R1" and "R2" was assessed using again a mixed-ANOVA test (between subjects factor: drivers R1/R2; within subjects factor: tasks). In order to assess significant differences between single tasks, one-way repeated measures ANOVA was used between all tasks (again PAC of each electrode as the dependent variable); drivers and copilots were analysed separately.

2.3.2 Stimulus Reconstruction

Only stimulus reconstruction coefficients with a statistically significant correlation to the original stimulus (Pearson's Rho <0.05) were analyzed. In order to find out if the reconstruction was sensitive enough to distinguish between tasks A, B and C (thus distinction between different attentional demand), an additional statistical analysis was performed.

First, the number of available coefficients was truncated to the lowest denominator of the tasks to compare (e.g. if task B was the task with the least coefficients, only the same number of coefficients from A and C were used). Then, all tasks (A, B, C) were compared using a linear regression model fit in MATLAB, where the independent variable was the task. Finally, to increase the robustness of the results, a repeated-measures analysis of variance (ANOVA) was performed in Excel, again to find out if there was a significant difference between reconstruction in tasks A, B or C.

3 Results

3.1 EEG Phase/Amplitude Coupling in a Driving Situation

3.1.1 Behavioral Data (Detection Task)

The task results (percentage of target words detected) are shown in Table 3.1 and represent the bevarioral data of the study. Repeated measures ANOVA was performed to compare the results (in % of correct button pressings per task) between audio training, task A and C (and their re-tests). For each group (drivers R1, drivers R2, copilots R1 and copilots R2), the difference between tasks was significant (all $p<0.001$ except copilot R2 $p=0.0079$). Additionally, the difference between drivers and copilots was studied for significance (drivers R1 against copilots R1 and drivers R2 against copilots R2). The group difference for R1 was significant ($p=0.0366$); the group difference for R2 did not reach significance ($p=0.2176$).

Table 3.1: Mean task results (in %) for the auditory task

Group	Audio Training	A	2A	C	2C
Drivers R1	83.5	48.9	50.2	39.7	37.6
Drivers R2	82.1	56	57.3	47.6	46
D R1 + R2	82.8	52.4	53.8	43.7	41.8
Copilots R1	78.7	67.1	67.1	55.6	56.6
Copilots R2	88.3	66.7	65.8	54.5	57.7
C R1 + R2	83.5	66.9	66.4	55	57.1

3.1.2 Phase-Amplitude Coupling

The results are shown for drivers and copilots, and afterwards, a sub-grouping of the drivers will be shown as well (Drivers "R1" against Drivers "R2").

Figure 3.1 shows the PAC results for all drivers (R1 and R2 combined), and all copilots (R1 and R2 combined), for all tasks. Figures 3.2 and 3.3 show the PAC results for baseline and training stages. Notice the scale for the training plots has been increased; shorter measurements produced higher PAC indices. Results for drivers R1 and R2 separately are shown in Figure 3.4.

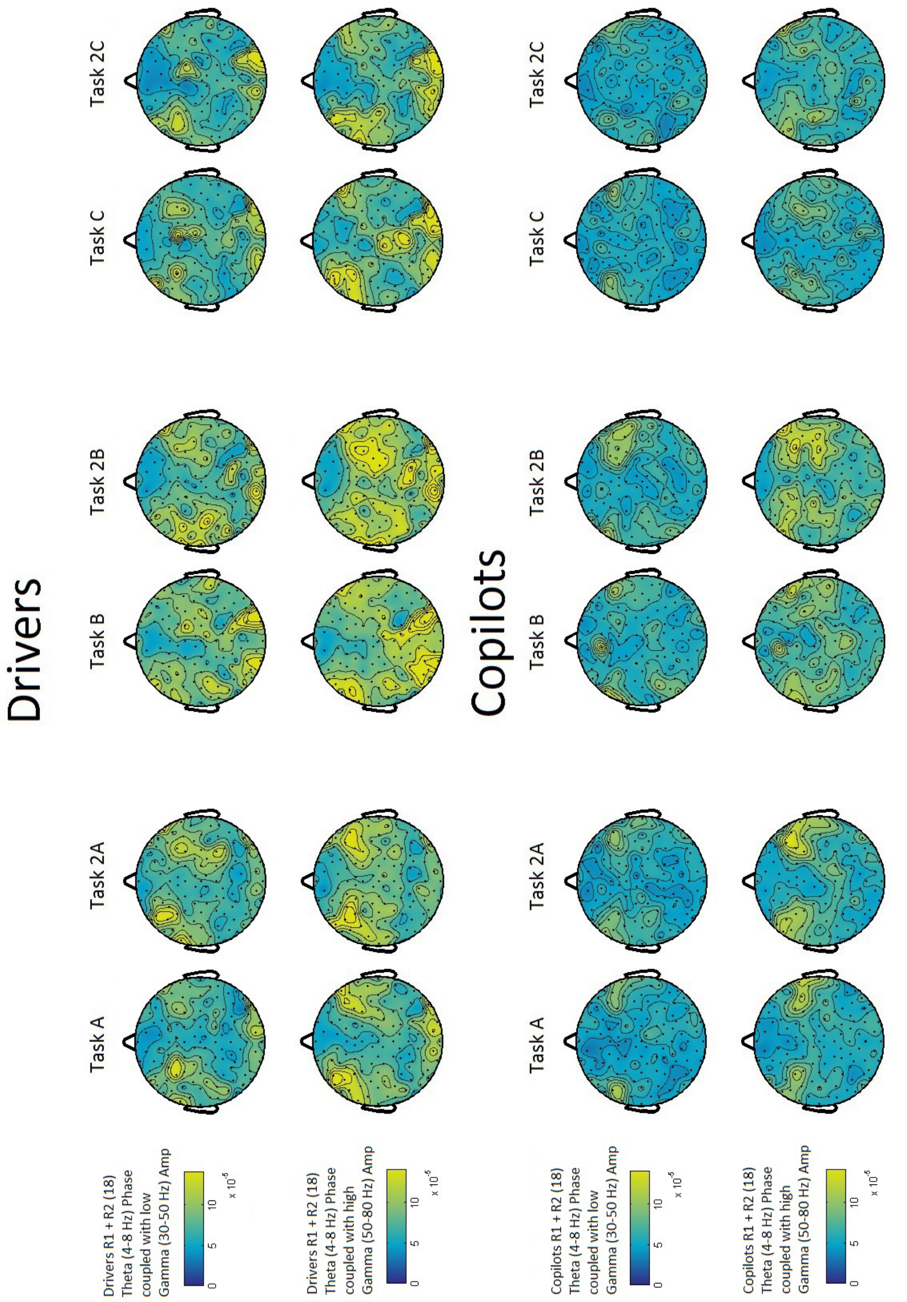

Figure 3.1: PAC results for all driver and copilots, main tasks. Modulation index is truncated to 0.00014 for clarity. Low (above) and high (below) Gamma amplitudes are shown, for all tasks.

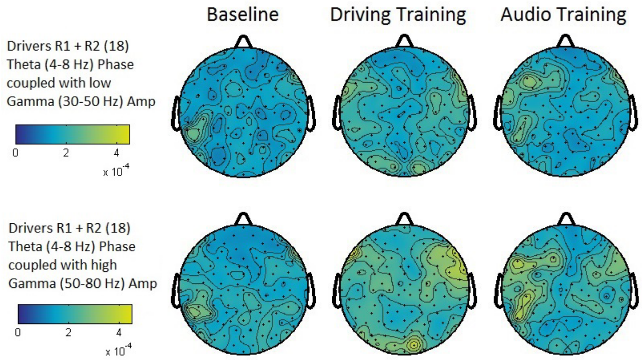

Figure 3.2: PAC results for all drivers (18), baseline/training tasks. Modulation index is truncated to 0.00045 (due to the decreased length of the measurement in the training stages). Low (above) and high (below) Gamma amplitudes are shown, for all tasks.

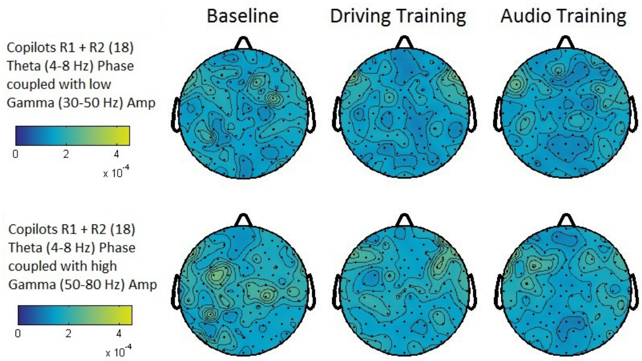

Figure 3.3: PAC results for all copilots (18), baseline/training tasks. Modulation index is truncated to 0.00045 (due to the decreased length of the measurement in the training stages). Low (above) and high (below) Gamma amplitudes are shown, for all tasks.

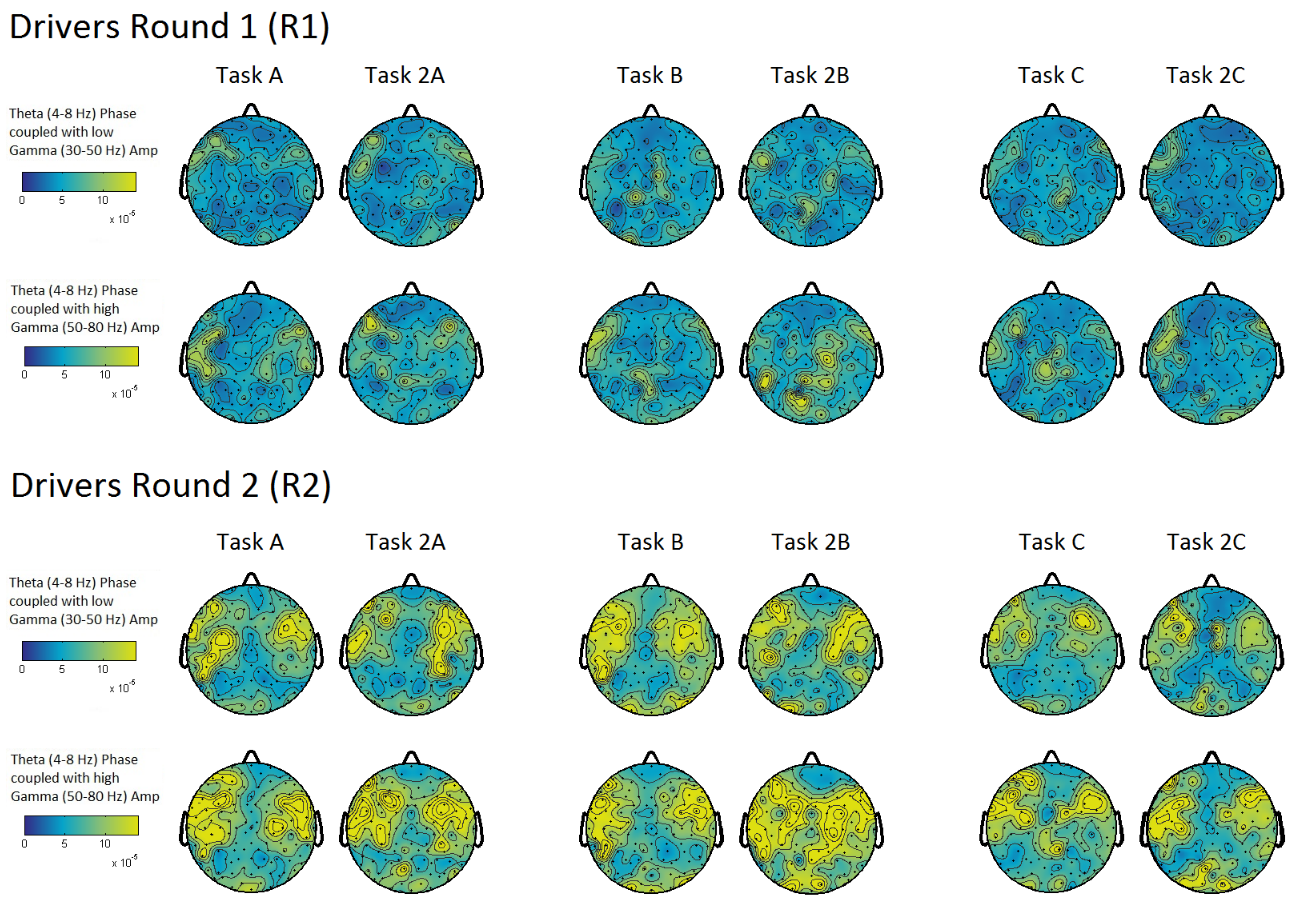

Figure 3.4: PAC results for drivers from rounds 1 and 2 separately. Modulation index is truncated to 0.00014 for clarity. Low (above) and high (below) Gamma amplitudes are shown, for all tasks.

3.1.3 Statistical Analysis - PAC

Nine regions of interest (ROIs) were defined to present the results: dorsolateral prefrontal cortex left (DLPFC L) and right (DLPFC R), frontal eye fields left (FEF L) and right (FEF R), superior frontal gyrus (SFG), primary motor cortex left (PMC L) and right (PMC R) and primary visual cortex left (PVC L) and right (PVC R). The electrodes that presented significant differences in the statistical analysis were grouped into each ROI and counted. The ROIs are shown in Fig. 3.5 and the number of electrodes with significant differences are shown in Table 3.2 and in graphical form in Fig. 3.6.

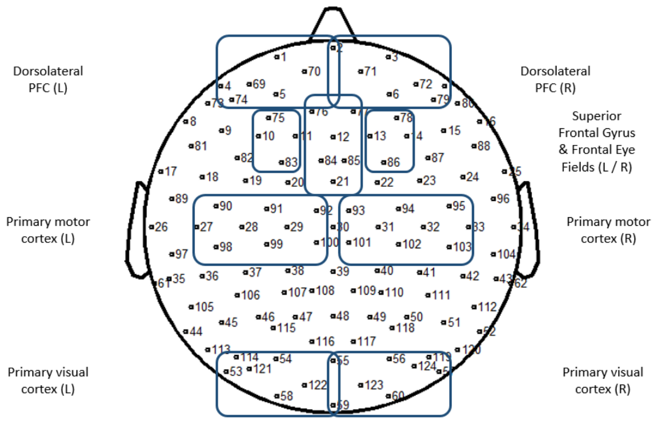

Figure 3.5: Regions of interest defined for the statistical studies

Given the results from repeated measures ANOVA, significant differences between the first and second round of each task were additionally investigated using a paired-T test. Results are shown in Figure 3.7, both for drivers and copilots.

Table 3.2: Number of electrodes with significant differences for each region of interest (ROI)

Statistics	R1	R2	R3	R4	R5	R6	R7	R8	R9
Low Gamma									
Mixed ANOVA BSF-R1 (drivers vs copilots)	0	0	0	0	0	0	1	2	1
Mixed ANOVA WSF - R1 (tasks)	1	2	1	1	0	1	1	0	0
Mixed ANOVA BSF-R1 vs R2 (drivers R1 vs drivers R2)	1	1	0	0	0	1	0	0	0
Mixed ANOVA WSF - R1 vs R2 (tasks)	0	2	0	0	0	1	0	0	0
RM ANOVA between tasks - all drivers	1	2	0	0	0	1	1	0	0
RM ANOVA between tasks - all copilots	0	0	0	2	0	0	0	1	0
High Gamma									
Mixed ANOVA BSF-R1 (drivers vs copilots)	0	0	0	0	0	1	0	0	1
Mixed ANOVA WSF - R1 (tasks)	0	1	2	2	2	4	6	1	1
Mixed ANOVA BSF-R1 vs R2 (drivers R1 vs drivers R2)	0	0	0	0	0	1	0	0	0
Mixed ANOVA WSF - R1 vs R2 (tasks)	0	1	0	2	0	0	4	0	1
RM ANOVA between tasks - all drivers	0	1	0	2	0	0	5	0	1
RM ANOVA between tasks - all copilots	0	0	0	0	0	2	2	3	0

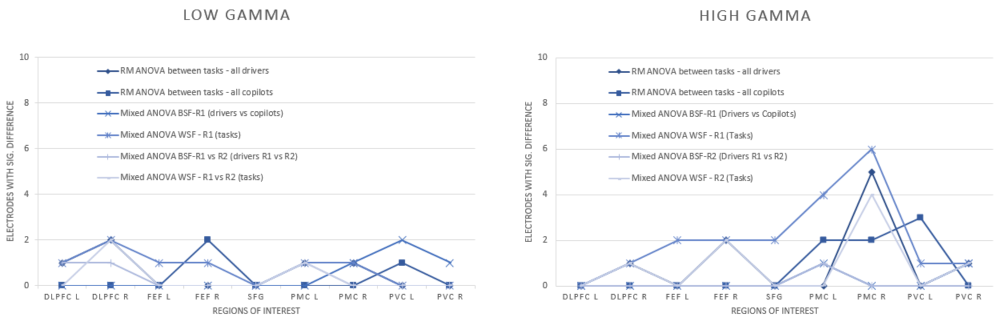

Figure 3.6: Number of electrodes with significant differences per study. The regions of interest are dorsolateral prefrontal cortex left (DLPFC L) and right (DLPFC R), frontal eye fields left (FEF L) and right (FEF R), superior frontal gyrus (SFG), primary motor cortex left (PMC L) and right (PMC R) and primary visual cortex left (PVC L) and right (PVC R).

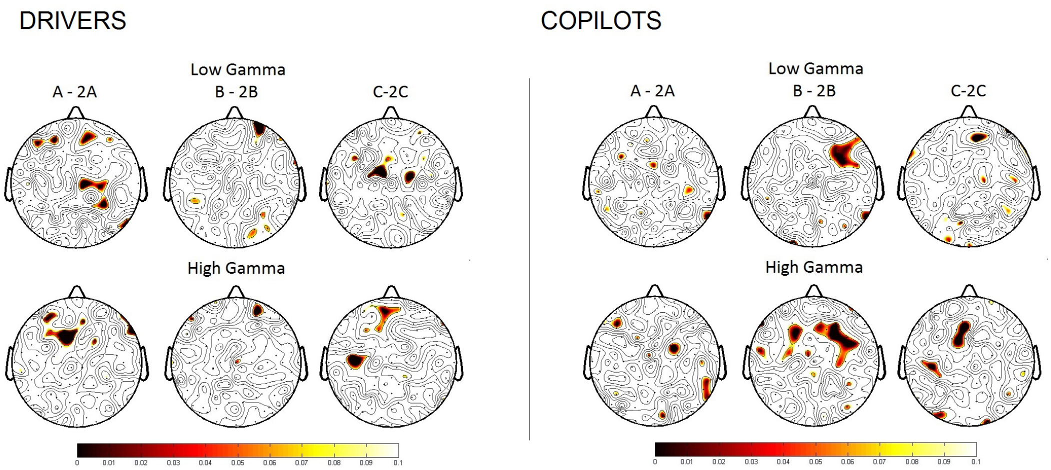

Figure 3.7: Paired-T Test results between test and re-test of each task, for low (above) and high (below) Gamma.

3.1.4 EEG Band Power

The band power analysis was calculated as a reference value, since it is often used to study brain activity. While no significant differences were found, the results are nevertheless presented for Drivers A (Figure 3.8), Drivers B (Figure 3.9), Copilots A (Figure 3.10) and Copilots B (Figure 3.11).

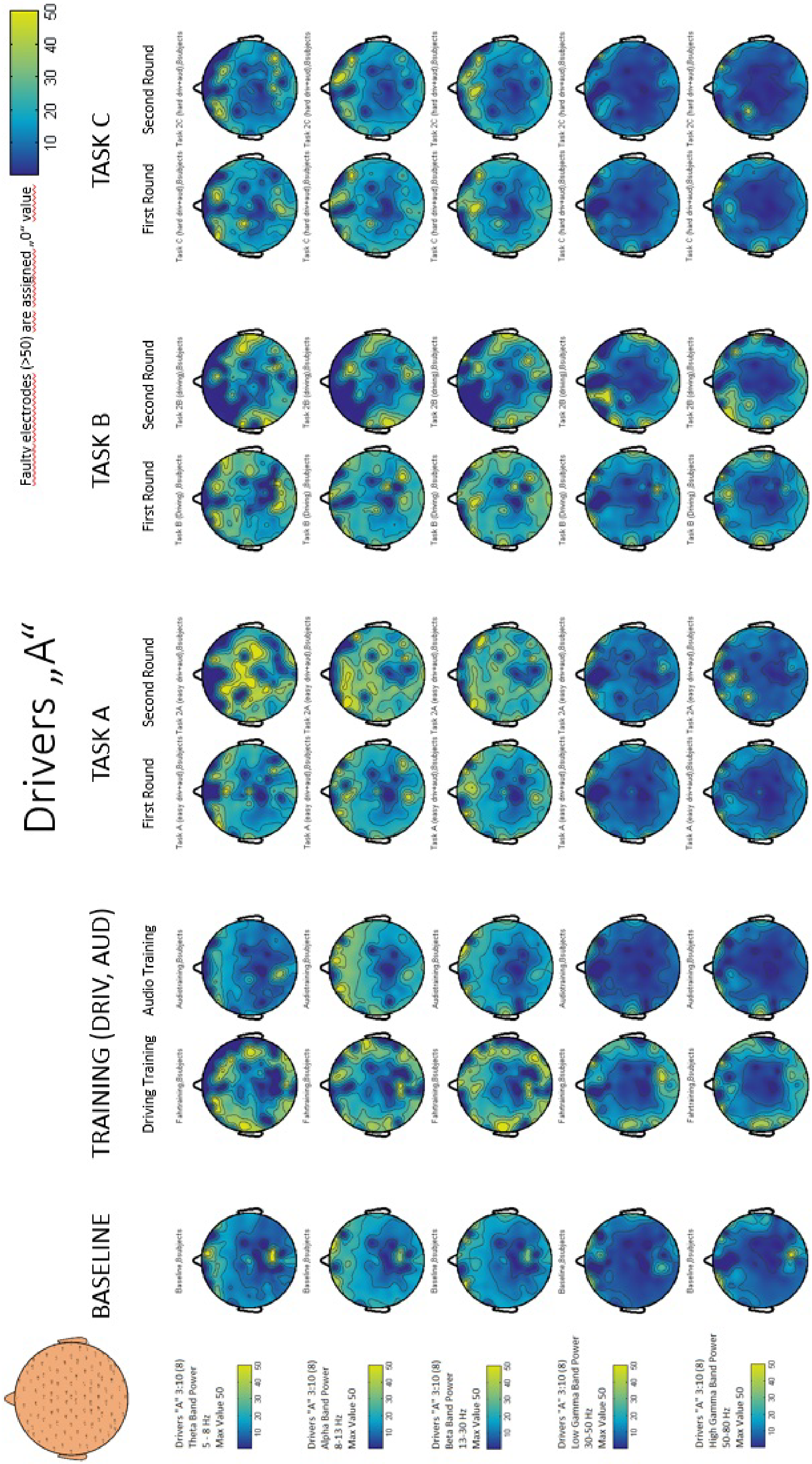

Figure 3.8: Band power analysis - Driver A

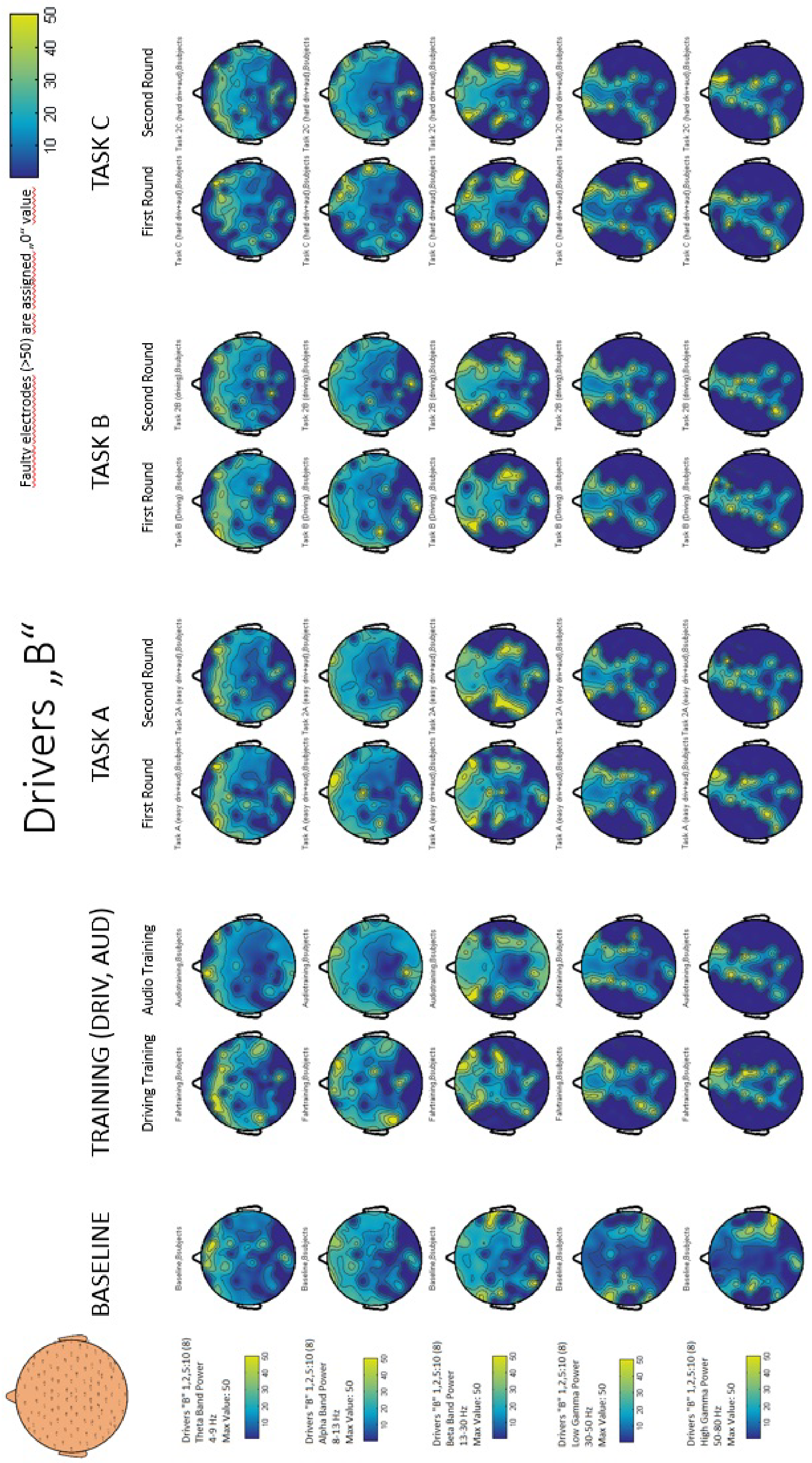

Figure 3.9: Band power analysis - Driver B

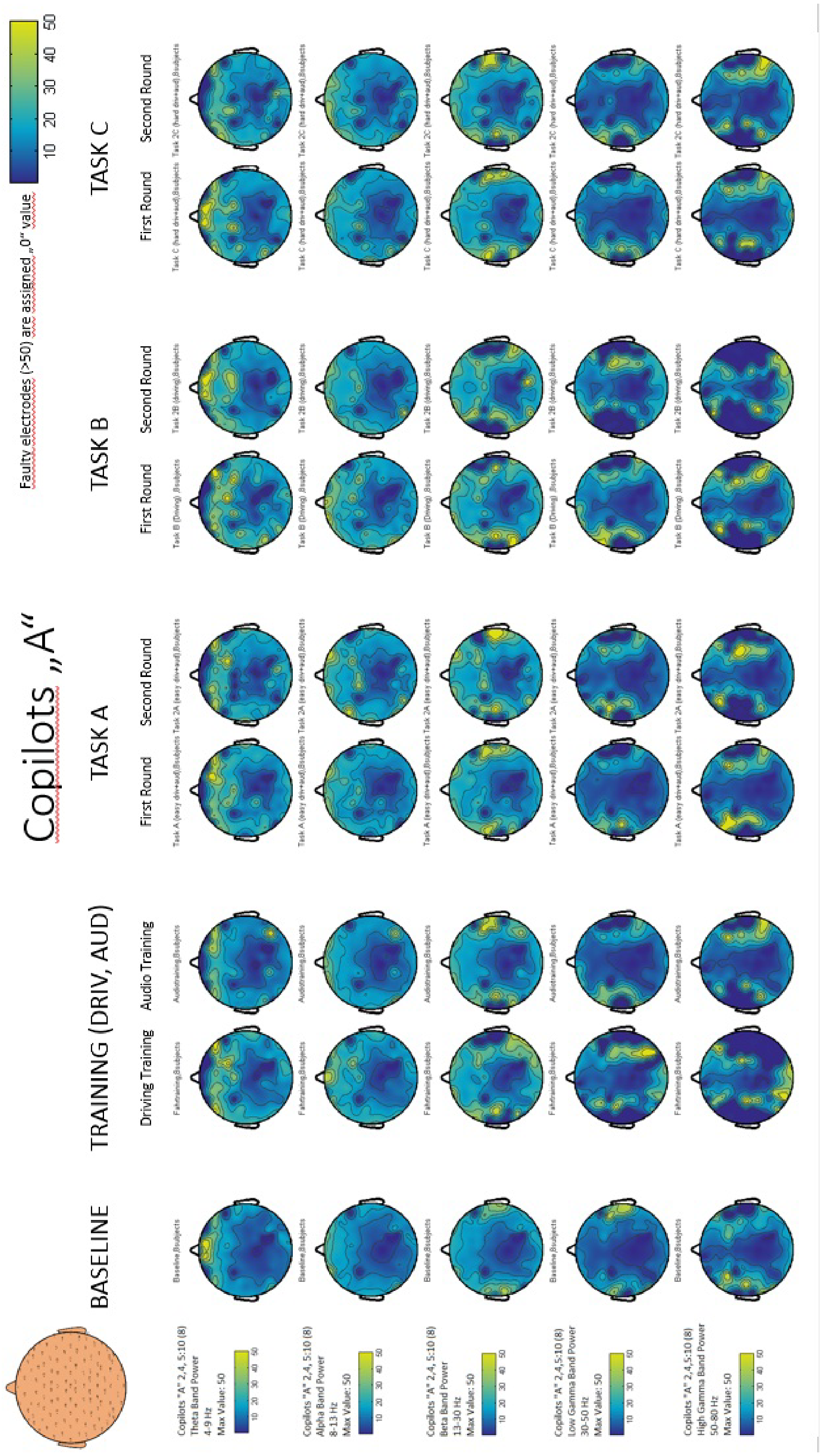

Figure 3.10: Band power analysis - Copilot A

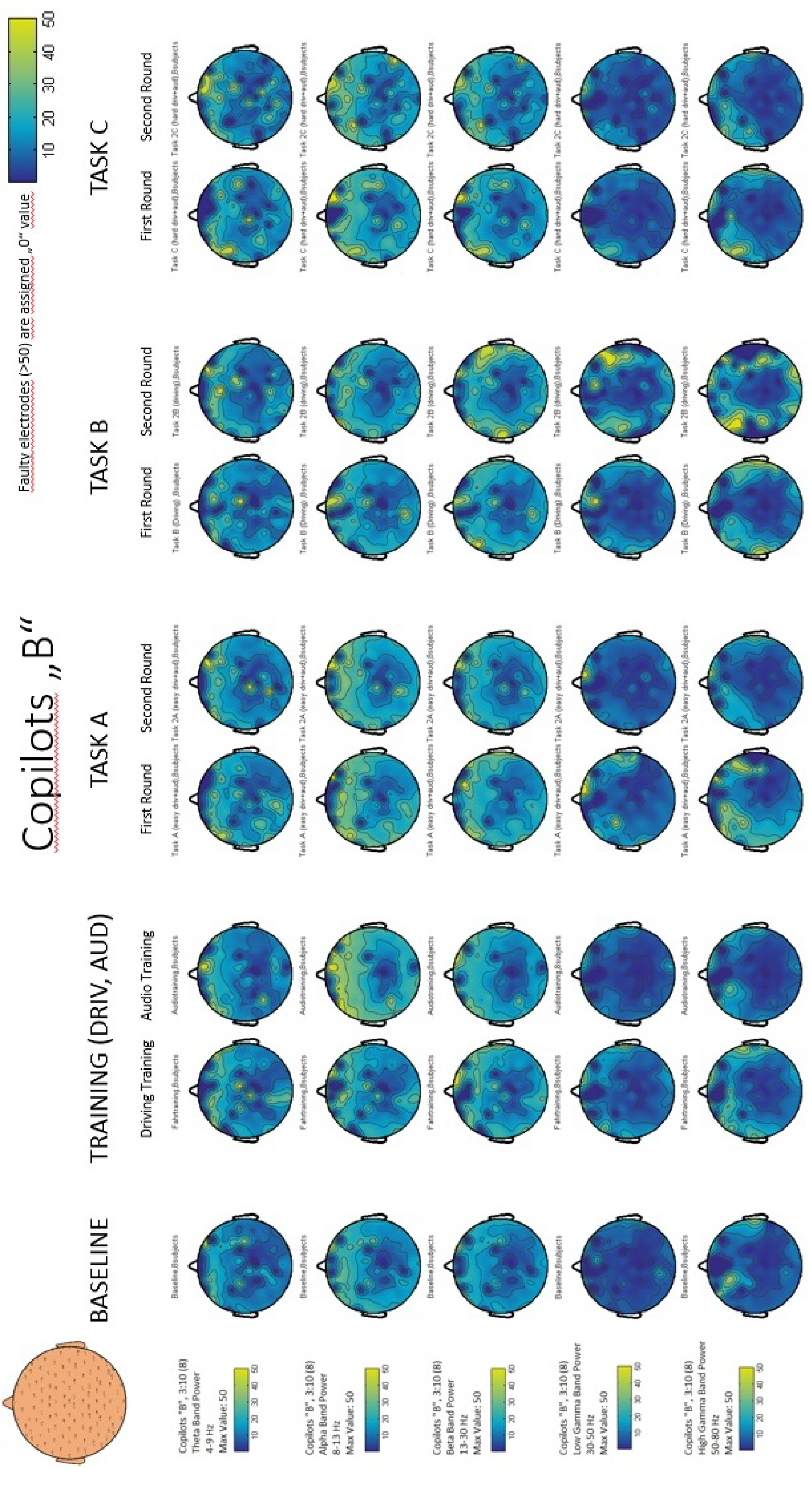

Figure 3.11: Band power analysis - Copilot B

3.2 Additional Research Work

3.2.1 Stimulus reconstruction accuracy

Fig. 3.12 shows the mean stimulus reconstruction accuracy for tasks A, B and C in round 1 (first time measurement), presented for drivers AND copilots, only drivers, and only passengers; Fig. 3.13 shows the same results for round 2 and Fig. 3.14 shows the overall results (combination of round 1 and 2).

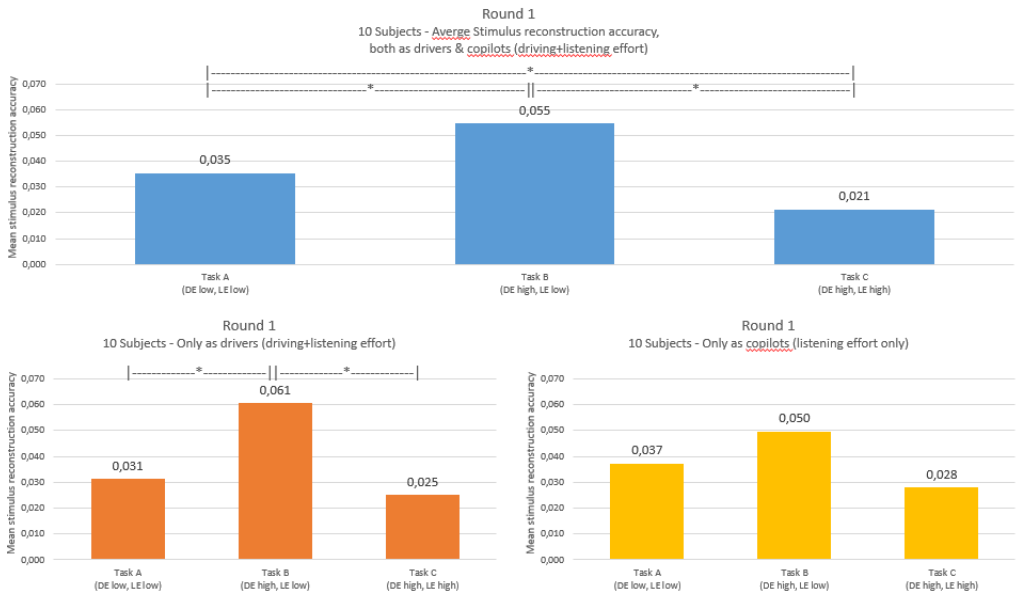

Figure 3.12: Round 1: Mean stimulus reconstruction accuracy values in tasks A (low driving and auditory effort), B (high driving effort, low auditory effort) and C (both driving and auditory effort high) for: (top) subjects both as driver and copilot; (lower left) only as driver; (lower right) only as copilot . Significant differences between tasks (p<0.05) denoted by asterisk (*); no significant difference between tasks for â€œonly as copilot". Overall, a better reconstruction is achieved whenever listening effort is the lowest (tasks A, B) and the best whenever no behavioral task (word detection) is involved (B).

3.2.2 Statistical analysis - stimulus reconstruction

The analysis in MATLAB using the linear regression model showed a significant difference (p<0.05) between tasks A, B and C. The analysis in Excel using repeated measures ANOVA confirmed the results seen in the linear model. Table 3.3 shows available re-

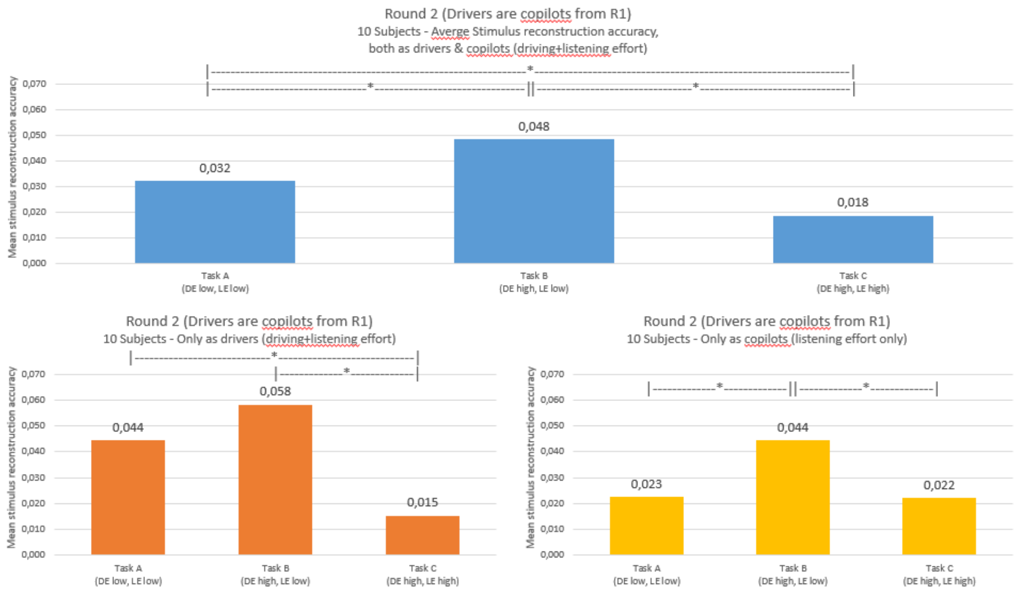

Figure 3.13: Round 2: Mean stimulus reconstruction accuracy values. Significant differences between tasks (p<0.05) denoted by asterisk (*). In the second round, the accuracy during task 1 for drivers increased, likely due to their experience as passengers during round 1.

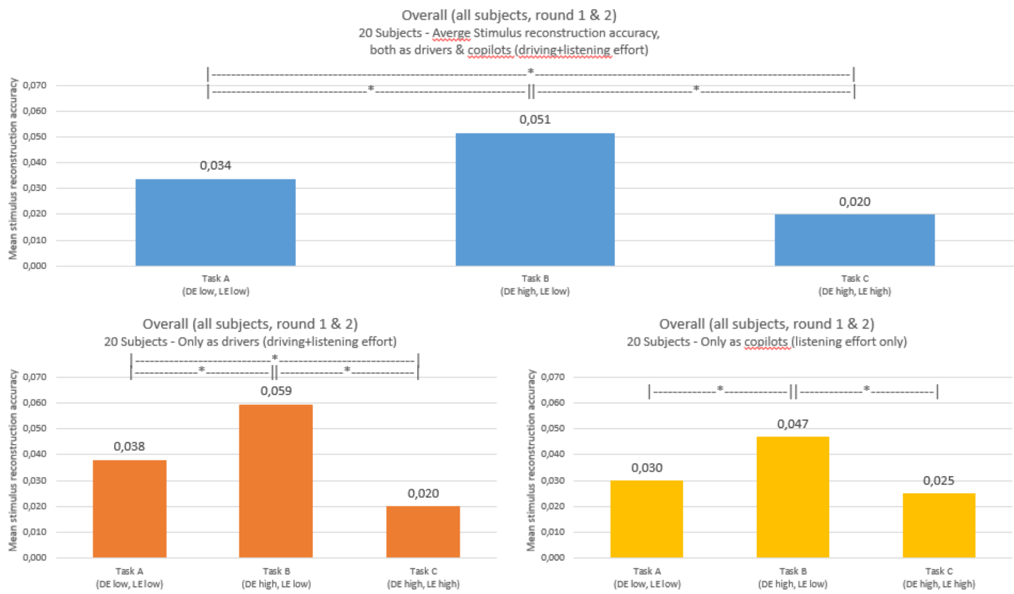

Figure 3.14: Rounds 1 and 2 analyzed together: Mean stimulus reconstruction accuracy values. Significant differences between tasks (p<0.05) denoted by asterisk (*). Tasks with low listening effort requirements presented higher reconstruction accuracy overall (A, B).

sults for both the linear regression model and ANOVA; significant differences (p<0.05) between tasks are denoted with an asterisk.

Table 3.3: Statistical analysis (linear regression model fit and repeated measures ANOVA)

	Linear model		RM ANOVA	
	P-Value	F-Value	P-Value	F-Value
Round 1				
Driver and copilot*	<0.001	12.728	<0.001	12.478
Driver only*	0.001	6.959	<0.001	7.655
Copilot only*	0.062	2.811	0.058	2.908
Round 2				
Driver and copilot*	<0.001	10.307	<0.001	11.897
Driver only*	<0.001	11.377	<0.001	12.996
Copilot only*	0.028	2.811	0.023	3.888
Overall				
Driver and copilot*	<0.001	23.029	<0.001	24.408
Driver only*	<0.001	16.572	<0.001	18.459
Copilot only*	0.002	6.150	0.002	6.509

Only after determining this did we use paired T-Tests to determine differences between tasks (A vs B, A vs C and B vs C). Significant differences as detected by the T-Test ($p<0.05$) are presented in Table 3.4 and denoted by asterisks in previous Figures 3.12, 3.13 and 3.14.

Table 3.4: Statistical analysis (Paired T-test)

	A vs B	A vs C	B vs C
Round 1			
Driver and copilot*	0.001	0.024	<0.001
Driver only	0.001	0.268	<0.001
Copilot only	no sig. diff. in lin.reg/ANOVA		
Round 2			
Driver and copilot*	0.004	0.013	<0.001
Driver only	0.056	0.001	<0.001
Copilot only	0.013	0.476	0.009
Overall			
Driver and copilot*	<0.001	0.001	<0.001
Driver only*	<0.001	0.004	<0.001
Copilot only	0.005	0.22	<0.001

4 Discussion

4.1 Main work

4.1.1 Behavioral Task

The results of the behavioral task are shown in Table 3.1. The highest scores were seen in the audio training stage (without driving) and the lowest in the Stage C (bad weather conditions mixed with solving the auditory detection task). Moreover, the test-retest reliability was also validated by the results of the behavioral task: results between first and second round of each stage (A-2A and C-2C) are almost identical.

4.1.2 Phase-Amplitude Coupling

The average results shown in Fig. 3.1 show the highest phase-amplitude coupling in the task B/2B (higher driving effort due to weather conditions, no auditory task), especially in the parietal and occipital areas. This suggests allocation of attention to the motor and visual areas of the cortex in the absence of auditory targets and supports the main hypothesis of the study.

Tasks A and C are characterized by coupling in the occipital areas (not as strong as in task B) and in the case of task C, a stronger coupling overall (task C combining driving and auditory tasks). It can be argued that the reduced PAC in the occipital areas of task C compared to task B obeys a reduction in the attentional resources available, which cannot be allocated exclusively to the one task and instead move back and forth according to the situation.

The PAC results for baseline and training are very low / non-existent. While the minimum measurement length for PAC algorithm to work was observed (and training / baseline scenarios were long enough for the algorithm to work), no clear PAC is visible. This might indicate the lack of a need for sustained attention.

Based on previous studies (Gonzalez-Trejo et al., 2013), activation in or around the auditory cortex was expected for the auditory training stage (as there was no other stimuli or task); however, no PAC was visible around the auditory cortex, neither for drivers nor for copilots. Neither was PAC seen for the tasks involving the auditory task (A and C). The secondary hypothesis regarding PAC around the auditory cortex could thus not be confirmed. Future work might tackle this finding (or lack of it). The area around the auditory cortex presents a challenge for high-resolution electrode systems since the electrode placement around the ear can be tricky. However, the impedance check during the measurement confirmed that electrodes of interest around the auditory cortex were placed correctly. Moreover, the results of the additional work (stimulus reconstruction) were able to obtain data regarding auditory attention using the same EEG dataset.

When comparing the drivers from the first round to the drivers from the second round (re-test, Fig. 3.4), a higher PAC was visible in all tasks. The same patterns of cortical activity are seen as in the results for all drivers together (predominant occipital activity in the task B, activity around motor cortex and frontal eye fields for all tasks). It can be argued that in the second round, the driver knows already what to expect and is able to allocate his or her attention more efficiently, therefore increasing the coupling seen.

4.1.2.1 High Gamma Band Activity in Surface EEG

Based on the PAC topographical maps and the number of electrodes with statistically significant PAC differences (Fig. 3.2), one of the secondary hypothesis was confirmed. Even with surface EEG, Gamma information up to 80 Hz was obtained and moreover, the coupling seemed to be stronger between Theta and High Gamma as seen in all topographic maps and in the number of electrodes with significant PAC differences. This invites to discuss the reports of Canolty et al. (2006); Jensen and Colgin (2007) regarding limits of surface EEG data (80 Hz); it would be interesting to test even higher Gamma frequencies to find the limit for PAC between Theta and Gamma components. Our results would thus recommend using the Gamma frequency band between 50 and 80 Hz for PAC.

4.1.2.2 Drivers Compared to Copilots

The occipital PAC seen in drivers is absent from copilots (overall, copilots present lower PAC); however an activation around the frontal eye fields can be seen specially in task B. Since copilots were not required to solve any kind of task, their attentional requirements were lower compared to the drivers. Moreover, as seen during the measurements, copilots had to be reminded constantly to keep their eyes on the road, which also suggests reduced attention / interest in the task and therefore reduced PAC. There was no significant differences in PAC from the copilot between test and retests or between round A and B (round B meaning that the copilot was the driver in the previous round).

4.1.2.3 Band Power Analysis

Band power analysis was performed for each task, for each task, for each condition and each round (including test-retest and drivers/copilots A and B, Figs. 3.8, 3.9, 3.10, 3.11). Theta, Alpha, Beta, low and high Gamma were all studied using bandpower function of MATLAB. No significant differences in activation were found. Moreover, the band power analysis was more susceptible to influence from artifacts; as seen in the figures, several electrodes had to be discarded due to reporting values above an acceptable threshold. As mentioned in Wascher et al. (2016), band power analysis might both correlate to mental effort, workload or fatigue; increase of alpha activity has been correlated to a reduction in performance (Sauseng et al., 2005) and a decrease has been correlated to increase of task complexity (Borghini et al., 2014). None of these changes were visible in the band power analysis, for any of the tasks presented.

4.2 Summary of PAC Results

The primary hypothesis of this work was to test the feasibility of phase amplitude coupling as a biomarker of attention in multimodal tasks such as a driving situation. As seen in the results, PAC allowed to identify cortical areas activated during specific tasks. Moreover, a clear difference between drivers and copilots was seen, allowing a differentiation between active and passive (or non-existent) attention in a driving situation. Certain parameters allowed a clearer PAC study; the high Gamma frequency window (50-80 Hz) delivered the best results.

The choice of Theta and Gamma bands and the results demonstrating a coupling between these bands agree with current state of the art research, where the regulation of competition between auditory and visual stimuli has been suggested to depend on Theta oscillations in the frontal cortex (Cavanagh and Frank, 2014; Wang et al., 2016), acting as modulators in feedback loops between other cortical regions and playing a role in top-down control (Cohen and Donner, 2013). An occipital Gamma-band activity (in visual cortical regions) has been linked to enhancements in visual attention (Green et al., 2017), which in this case could be regulated by Theta activity.

The setup proved to be flexible enough to study a new paradigm. The choice of PAC was adequate as it allowed to study the cognitive effort while multitasking (driving, solving an auditory task) in real time. Setup optimizations can allow to test the paradigm in real life situations. There are different ways to study PAC, but as seen in the review analysis from Hülsemann et al. (2019), using the modulation index (MI) as in this thesis seems to be the most robust way to calculate the coupling, especially in noisy and short signals.

Applications of the current results can be seen in neuroergonomics (i.e. effects of neuroscience in human performance, specifically while driving). Given the trend for vehicles to depend less on the subject (e.g. Autopilot), a reliable way to monitor the attention of the subject could support the vehicle systems in decision making (e.g. to determine if the driver needs to take control of the wheel in a given situation and if he/she is actually capable to do it at a given time). As studied by Solis-Marcos et al. Solis-Marcos et al. (2017) demonstrated that automation levels in vehicles affected the attention of the driver even after short periods of driving. Therefore, current technology and infrastructure still requires for the driver to react in case of an emergency, and quantifying the attention of the driver at any given time could prove useful. An application example would be to define an area of interest within the cortex and only monitor this area; thus reducing the number of electrodes and data processing necessary to measure PAC and interpret it in the context of the task. The tools developed for the data acquisition and analysis should also be flexible enough to be used with other paradigms involving high resolution EEG.

Phase amplitude coupling is turning to be a popular approach for studying EEG frequency band dynamics; a PUBMED search (January 2021) with the keywords "phase amplitude coupling" returns 376 articles, 72 alone in 2020. The topics in which PAC has found an application range from speech processing (Lizarazu et al., 2019), visual attention (Tzvi et al., 2018), memory retrieval and consolidation (Mikutta et al., 2019; Bergmann and Born, 2018), Parkinson's disease, autism, seizures (Ibrahim et al., 2018), among others (only the publications that used the same PAC methodology as the one presented by the author in this work are cited). More theoretical frameworks have also seen the application of PAC, such as the study of local field potentials and their direction (Nandi et al., 2019).

Shortcomings of the current study include the preparation time, which can extend for hours given the driver/copilot setting (each having 128 EEG electrodes plus electrooculogram and other sensors), the reliability of the EEG electrodes (the head does not remain static in a driving task and the EEG array should not be affected by movement of the head) and the reduced number of subjects. Moreover, while the behavioral task offered a comparison to alternative attentional measurements while driving, PAC can still be compared and validated against other established tools, such as fNIRS or MEG - this was not possible with the current setup.

4.2.1 PAC - Future Work

Miniaturization of the setup should be a goal for future work: finding out the minimum number of electrodes necessary to assess PAC while driving can lead to a setup/paradigm that can be tested in real settings (the current setup can be tested already but requires long preparation times due to the 2x128 electrode arrays and needs to be taken care of constantly to ensure correct functioning and data acquisition). The limit for Gamma frequency as reported in the literature were strictly observed; however, it remains to be seen if Gamma information past 80 Hz as seen in surface EEG can still be useful for PAC.

Finally, based on the lack of PAC around the auditory cortex when solving a pure auditory task, it would be interesting to measure PAC in a more controlled environment, where only an auditory task (can even be the same as in the driving simulator) has to be solved; a 2-channel setup as in the ground work could be used to target the auditory cortex more specifically and use these results to conclude if the electrode placement during the driving task might have influenced the lack of results. The presence of PAC in the auditory cortex was recently proven by Lizarazu et al. (2019), who used PAC (also between Theta and Gamma) to study speech processing and brain adaptations to speech rate. While they did not use EEG but magnetoencephalography, they were able to observe PAC in both the left and right auditory cortex. This would either point to a limitation within EEG or the setup used for the current work.

4.3 Additional Research Work

4.3.1 Stimulus Reconstruction Accuracy

As seen in Figs. 3.12, 3.13 and 3.14, a higher reconstruction accuracy is achieved in a low listening effort condition (such as A or B). This suggests that the lack of auditory distractors, even in the presence of increase driving effort, allows the participant to focus on the auditory stream and thus the stream can be reconstructed with a higher success rate. As expected, Task C presented the lowest reconstruction accuracy result as the participants are faced with taxing attentional tasks (both driving and auditory tasks), which leave less resources available to follow the stream accurately and therefore reduce the success of the stimulus reconstruction. When splitting drivers and copilots into groups based on rounds (1 or 2), we observed a higher success in stimulus reconstruction results in all tasks drivers during Round 1 (naive drivers during the driving round) (Fig. 3.12) and lower during round 2 (Fig. 3.13). Thus the novelty of the scenario did play a role in stimulus reconstruction results and indicates a higher saliency / attention to the stimulus during the first round, whichever it was for each participant. The increased attention due to the novelty then allows for a more successful stimulus reconstruction. The attention to the podcast then decreases by the second round (after participants switch places) and therefore the stimulus reconstruction accuracy decreases as well, nevertheless remaining distinct for each scenario based on the effort required to follow the tasks.

4.3.2 Contribution to the Main Work

The original results of the PAC analysis presented beforehand reported an increased phase-amplitude coupling (PAC) specially during Task B (high driving effort, low auditory effort). However, the PAC analysis failed to find any auditory-related activation or coupling, even during high auditory effort (Task C) or auditory training. The stimulus reconstruction (which is focused on auditory tasks) used the same EEG data set for the same tasks in the same time interval and was able find statistically significant differences ($p<0.05$) between Tasks A, B and C, and moreover, to pinpoint scenario B as the one where the stimulus could be reconstructed with the highest accuracy. This applied for round 1, 2 and both combined.

Overall, Task B presents a higher driving effort in the form of traffic and adverse weather conditions within an urban environment, but there was no auditory task (the broadcast is playing but no word needs to be detected). The results suggest that attention increased due to the situation (high stress while driving) but since there is no auditory task (no button press, only playback of the broadcast), the stimulus reconstruction becomes easier (more attentional resources available). One could suggest that task A does not tax the attention enough so participants might not be focusing enough on the environment, while task C requires too much attention and does not allow to focus on the stream but instead on the single task word ("und"), thus hindering the reconstruction.

Thus, we were able to extract additional data from the EEG datasets used in the main work of this dissertation, and to obtain information regarding auditory attention that was not visible using the PAC method. Our results suggest that stimulus reconstruction works as an indicator of auditory effort as well (even in taxing, multimodal effort conditions) and can be used to complement results in datasets that were not originally prepared for this analysis.

5 Conclusions

This thesis work deals with the assessment of attention in complex, multimodal tasks such as driving, using novel tools to analyze electroencephalographic (EEG) data. The publication consisting the main work of this dissertation consisted on measuring the EEG of the driver while driving, combined with a behavioral task, in order to assess the cognitive effort and attentional demands. This effort was quantified by using the novel technique of phase-amplitude coupling (PAC), specifically observing coupling between Theta phase and Gamma amplitude. The results confirmed current state of the art research regarding roles of Theta and Gamma oscillations in cognitive performance during audiovisual tasks (see Cavanagh and Frank (2014); Wang et al. (2016); Cohen and Donner (2013); Green et al. (2017)); showed that PAC can accurately pinpoint cortical activation related to such cognitive effort and attention. Moreover, the author was able to show that copilots present different cortical activation as seen in PAC, compared to drivers. This could be characterized as the difference between active and passive cognitive load in a driving situation. The conception that the Gamma spectrum of EEG is limited by surface EEG was also tested; surface EEG was able to extract more relevant information from the Gamma interval between 50 and 80 Hz.

Results suggest the feasibility of PAC as a biomarker for cognitive effort in multimodal tasks. The method is sensitive enough to distinguish between drivers and copilots; can be measured while driving (unlike the ALR measurement presented in the ground work) and can be done in a portable way. Moreover, PAC has found more applications as of late in different fields of neurology (see Jensen and Colgin (2007); Cohen (2008); Jirsa and Müller (2013); Tort et al. (2010); Canolty et al. (2006); Lisman (2005); Dimitriadis et al. (2015); Bruns and Eckhorn (2004); Demiralp et al. (2007)). Thus, almost all postulated hypotheses were confirmed with the exception of the final secondary hypothesis: there was no increase in PAC on the auditory cortex.

The additional research work presented in this thesis served two purposes. First, it was able to reconstruct the auditory stimuli and thus provide an indicator of attentional demands during driving; moreover, it was sensitive enough to differentiate between the different tasks (increasing the information available from the same EEG set as the PAC measurement). It also validated the methods developed by our work group for stimulus reconstruction by being used in EEG data sets that were not acquired with stimulus reconstruction in mind.

To the authors knowledge, this is the first (and at the time of the publication of (Gonzalez Trejo et al., 2019) also the only) work dealing with PAC in driving situations, supporting the field of neuroergonomics and human-machine interfaces.

Future work might focus on testing the setup in real-life situations and on finding how real-time PAC analysis could serve as feedback in vehicles (e.g. detecting deviations in attention while driving); it might be also of interest to try reducing the number of electrodes needed to acquire the information and thus improve portability. Application in other fields of study is open and the tools developed for this thesis are available and easily adapted for new paradigms. Finally, the absence of PAC in the auditory cortex should be further evaluated, as it was not expected and the results did not offer enough insight on it.

Bibliography

Ahn, S., Nguyen, T., Jang, H., Kim, J. G., and Jun, S. C. (2016). Exploring neurophysiological correlates of drivers' mental fatigue caused by sleep deprivation using simultaneous EEG, ECG and fNIRS data. *Frontiers in Human Neuroscience*, 10(219):1–14.

Arrighi, P., Bonfiglio, L., Minichilli, F., Cantore, N., Carboncini, M. C., Piccotti, E., Rossi, B., and Andre, P. (2016). EEG theta dynamics within frontal and parietal cortices for error processing during reaching movements in a prism adaptation study altering visuo-motor predictive planning. *PLoS One*, 11(3):1–27.

Avery, M. C., Dutt, N., and Krichmar, J. L. (2014). Mechanisms underlying the basal forebrain enhancement of top-down and bottom-up attention. *European Journal of Neuroscience*, 39:852–865.

Battistoni, E., Stein, T., and Peelen, M. V. (2017). Preparatory attention in visual cortex. *Ann N Y Acad Sci*, 1396(1):92–107.

Bergmann, T. O. and Born, J. (2018). Phase-amplitude coupling: A general mechanism for memory processing and synaptic plasticity? *Neuron*, 97(1):10–13.

Bidet-Caulet, A., Bottemanne, L., Fonteneau, C., Giard, M. H., and Bertrand, O. (2015). Brain dynamics of distractibility: interaction between top-down and bottom-up mechanisms of auditory attention. *Brain Topography*, 28(3):423–436.

Borghini, G., Astolfi, L., Vecchiato, G., Mattia, D., and Babiloni, F. (2014). Measuring neurophysiological signals in aircraft pilots and car drivers for the assessment of mental workload, fatigue and drowsiness. *Neuroscience and Biobehavioral Reviews*, 44:58–75.

Boutros, N. N., Korzyukov, O., Jansen, B., Feingold, A., and Bell, M. (2004). Sensory gating deficits during the mid-latency phase of information processing in medicated schizophrenia patients. *Psychiatry Res*, 126(3):203–215.

Bowyer, S. M., Hsieh, L., Moran, J. E., Young, R., Manoharan, A., Liao, C. J., Malladi, K., Yu, Y., Chiang, Y. R., and Tepley, N. (2009). Conversation effects on neural mechanisms underlying reaction time to visual events while viewing a driving scene using MEG. *Brain Research*, 1251:151–161.

Bregman, A. S. (1990). *Auditory Scene Analysis*. MIT Press, Cambridge, MA.

Bruns, A. and Eckhorn, R. (2004). Task-related coupling from high- to low-frequency signals among visual cortical areas in human subdural recordings. *International Journal of Psychophysiology*, 51:97–116.

Buschman, T. J. and Kastner, S. (2015). From behavior to neural dynamics: an integrated theory of attention. *Neuron*, 88(1):127–144.

Buzsáki, G. and Draguhn, A. (2013). Neuronal oscillations in cortical networks. *Science*, 304(5679):1926–1929.

Calhoun, V. D., McGinty, V. B., and Pearlson, G. D. (2001). Driving and the brain: an imaging study. In *Proceedings of the 1st Human-Centered Transfortation Simulation Conference, The University of Iowa, November 2001 Iowa, United States of America*.

Calhoun, V. D. and Pearlson, G. D. (2012). A selective review of simulated driving studies: Combining naturalistic and hybrid paradigms, analysis approaches, and future directions. *NeuroImage*, 59:25–35.

Canolty, R. T., Edwards, E., Dalal, S. S., Soltani, M., Nagarajan, S. S., Kirsch, H. E., Berger, M. S., Barbaro, N. M., and Knight, R. T. (2006). High gamma power is phase-locked to theta oscillations in human neurocortex. *Science*, 313:1626–1628.

Cavanagh, J. F. and Frank, M. J. (2014). Frontal theta as a mechanism for cognitive control. *Trends Cogn Sci*, 18(8):414–421.

Cherry, E. (1953). Some experiments on the recognition of speech, with one and two ears. *J. Acoust. Soc. Amer.*, 25:975–979.

Chung, S. C., Choi, M. H., Kim, H. S., You, N. R., Hong, S. P., Lee, J. C., Park, S. J., Baek, J. H., Jeong, U. H., You, J. H., Lim, D. W., and Kim, H. J. (2014). Effects of distraction task on driving: a functional magnetic resonance imaging study. *Bio-Medical Materials and Engineering*, 24:2971–2977.

Cohen, M. X. (2008). Assessing transient cross-frequency coupling in EEG data. *Journal of Neuroscience Methods*, 168:494–499.

Cohen, M. X. (2011). Error-related medial frontal theta activity predicts cingulate-related structural connectivity. *NeuroImage*, 55:1373–1383.

Cohen, M. X. and Donner, T. H. (2013). Midfrontal conflict-related theta-band power reflects neural oscillations that predict behavior. *J Neurophysiol*, 110(12):2752–2763.

Connor, C. E., Egeth, H. E., and Yantis, S. (2004). Visual attention: Bottom-up versus top down. *Current Biology*, 14(19):R850–R852.

Corbetta, M. and Shulman, G. L. (2002). Control of goal-directed and stimulus-driven attention in the brain. *Nature Reviews Neuroscience*, 3:201–215.

Crosse, M. J., Di Liberto, G. M., Bednar, A., and Lalor, E. C. (2016). The multivariate temporal response function (mtrf) toolbox: A MATLAB toolbox for relating neural signals to continuous stimuli. *Frontiers in Human Neuroscience*, 10:604.

Demiralp, T., Bayraktaroglu, Z., Lenz, D., Junge, S., Busch, N. A., Maess, B., Ergen, M., and Herrmann, C. S. (2007). Gamma amplitudes are coupled to theta phase in human EEG during visual perception. *International Journal of Psychophysiology*, 64:24–30.

Desimone, R. and Duncan, J. (1995). Neural mechanisms of selective visual attention. *Annu. Rev. Neurosci.*, 18:193–222.

Dhamala, M., Assisi, C. G., Jirsa, V. K., Steinberg, F. L., and Kelso, J. A. (2007). Multisensory integration for timing engages different brain networks. *Neuroimage*, 34(2):764–773.

Dien, J. (1998). Issues in the application of the average reference: Review, critiques and recommendations. *Behavior Research Methods, Instruments & Computers*, 30:34–43.

Dimitriadis, S. I., Sun, Y., Kwok, K., Laskaris, N., Thakor, N., and Bezerianos, A. (2015). Cognitive workload assessment based on the tensorial treatment of EEG estimates of cross-frequency phase interactions. *Annals of Biomedical Engineering*, 43(4):977–989.

Duncan, J. and Humphreys, G. W. (1989). Visual search and stimulus similarity. *Psychol Rev*, 96(3):433–458.

Eimer, M. (2015). EPS Mid-Career Award 2014. The control of attention in visual search: Cognitive and neural mechanisms. *Q J Exp Psychol (Hove)*, 68(12):2437–2463.

Engel, A. K., Fries, P., and Singer, W. (2001). Dynamic predictions: Oscillations and synchrony in top–down processing. *Nature Review Neuroscience*, 2:704–718.

Escera, C., Alho, K., Schröger, E., and Winkler, I. (2000). Involuntary attention and distractability as evaluated with event-related brain potentials. *Audiol Neurootol*, 5(3-4):151–166.

Fastl, H. (1987). A background noise for speech audiometry. *Audiol. Acoustics*, 26:2–13.

Ferree, T. C. (2000). Calculation of average reference. *Electrical Geodesics Inc (Oregon, USA)*, pages 1–2. Technical Report from manufacturer.

Fort, A., Martin, R., Jacquet-Andrieu, A., Combe-Pangaud, C., Foliot, G., Daligault, S., and Delpuech, C. (2010). Attentional demand and processing of relevant visual information during simulated driving: A MEG study. *Brain Research*, 1363:117–127.

Fries, P. (2005). A mechanism for cognitive dynamics: neuronal communication through neuronal coherence. *TRENDS in Cognitive Sciences*, 9(10):474–480.

Gärtner, M., Rohde-Liebenau, L., Grimm, S., and Bajbouj, M. (2014). Working memory-related frontal theta activity is decreased under acute stress. *Psychoneuroendocrinology*, 43:105–113.

Gonzalez-Trejo, E., Hermann, D., Kohl, M., Corona-Strauss, F. I., and Strauss, D. J. (2013). Paired chirp evoked cortical inhibition and its behavioral correlates in a speech intelligibility task. In *Conf Proc IEEE Neural Engineering*, volume 2013:1, pages 1350–1353.

Gonzalez Trejo, E., Mögele, H., Pfleger, N., Hannemann, R., and Strauss, D. J. (2019). Electroencephalographic phase amplitude coupling in simulated driving with varying modality-specific attentional demand. *IEEE Transactions on Human-Machine Systems*. in press.

Green, J. J., Boehler, C. N., Roberts, K. C., Chen, L., Krebs, R. M., Song, A. W., and Woldorff, M. G. (2017). Cortical and subcortical coordination of visual spatial attention revealed by simultaneous EEG-fMRI recording. *J Neurosci*, 37(33):7803–7810.

Gruber, T., Müller, M. M., Keil, A., and Elbert, T. (1999). Selective visual-spatial attention alters induced gamma band responses in the human EEG. *Clinical Neurophysiology*, 110:2074–2085.

Grummett, T. S., Fitzgibbon, S. P., Lewis, T. W., DeLosAngeles, D., Whitham, E. M., Pope, K. J., and Willoughby, J. O. (2014). Constitutive spectral eeg peaks in the gamma range: supressed by sleep, reduced by mental activity and resistant to sensory stimulation. *Frontiers in Human Neuroscience*, 8(927):1–11.

Hagemann, D., Naumann, E., and Thayer, J. F. (2001). The quest for the eeg reference revisited: A glance from brain asymmetry research. *Psychophysiology*, 38:847–857.

Harris, A. M., Dux, P. E., Jones, C. N., and Mattingley, J. B. (2017). Distinct roles of theta and alpha oscillations in the involuntary capture of goal-directed attention. *NeuroImage*, 152:171–183.

Harris, K. D. and Thiele, A. (2012). Cortical State and Attention. *Nat Rev Neurosci*, 12(9):509–523.

Herrmann, C. S., Munk, M. H. K., and Engel, A. K. (2004). Cognitive functions of gamma-band activity: memory match and utilization. *TRENDS in Cognitive Sciences*, 8(8):347–355.

Horrey, W. J. and Wickens, C. D. (2004). Driving and side task performance: the effects of display clutter, separation, and modality. *Human Factors*, 46(4):611–624.

Hülsemann, M. J., Naumann, E., and Rasch, B. (2019). Quantification of phase-amplitude coupling in neuronal oscillations: Comparison of phase-locking value, mean vector length, modulation index, and generalized-linear-modeling-cross-frequency-coupling. *Front Neurosci*, 13(1):573.

Hyvärinen, A. and Oja, E. (2000). Independent component analysis: algorithms and applications. *Neural Networks*, 13:411–430.

Ibrahim, G. M., Wong, S., Morgan, B. R., Lipsman, N., Fallah, A., Weil, A. G., Krishna, V., Wennberg, R. A., and Lozano, A. A. (2018). Phase-amplitude coupling within the anterior thalamic nuclei during seizures. *J Neurophysiol*, 119(4):1497–1505.

Jap, B. T., Lal, S., Fischer, P., and Bekiaris, E. (2009). Using EEG spectral components to assess algorithms for detecting fatigue. *Expert Systems with Applications*, 36:2352–2359.

Jensen, O. and Colgin, L. L. (2007). Cross-frequency coupling between neuronal oscillations. *TRENDS in Cognitive Sciences*, 11(7):267–269.

Jensen, O., Kaiser, J., and Lachaux, J. P. (2007). Human gamma-frequency oscillations associated with attention and memory. *TRENDS in Neurosciences*, 30(7):317–324.

Jirsa, V. and Müller, V. (2013). Cross-frequency coupling in real and virtual brain networks. *Frontiers in Computational Neuroscience*, 7(78):1–25.

Johansson, M. (1999). The hilbert transform. Master's thesis, Växjö University.

Just, M. A., Keller, T. A., and Cynkar, J. (2008). A decrease in brain activation associated with driving when listening to someone speak. *Brain Research*, 1205:70–80.

Kan, K., Schweizer, T. A., Tam, F., and Graham, S. J. (2013). Methodology for functional MRI of simulated driving. *Medical Physics*, 40(1).

Kasper, R. W., Grafton, S. T., Eckstein, M. P., and Giesbrecht, B. (2015). Multimodal neuroimaging evidence linking memory and attention systems during visual search cued by context. *Ann N Y Acad Sci*, 1339(1):176–189.

Katsuki, F. and Constantidinis, C. (2014). Bottom-up and top-down attention: Different processes and overlapping neural systems. *The Neuroscientist*, 20(5):509–521.

Katsuki, F. and Constantinidis, C. (2012). Unique and shared roles of the posterior parietal and dorsolateral prefrontal cortex in cognitive functions. *Frontiers in integrative neuroscience*, 6(17):1–13.

Katus, T., Grubert, A., and Eimer, M. (2017). Intermodal Attention Shifts in Multimodal Working Memory. *J Cogn Neurosci*, 29(4):628–636.

Katzuki, F. and Constantinidis, C. (2014). Bottom-up and top-down attention: Different processes and overlapping neural systems. *The Neuroscientist*, 20(5):509–521.

Kirschfeld, K. (2005). The physical basis of alpha waves in the electroencephalogram and the origin of the "Bergere effect". *Biological Cybernetics*, 92:177–185.

Klimesch, W. (1999). EEG alpha and theta oscillations reflect cognitive and memory performance: A review and analysis. *Brain Research Reviews*, 29:169–195.

Koch, C. and Ullman, S. (1985). Shifts in selective visual attention: towards the underlying neural circuitry. *Hum Neurobiol*, 4(4):219–227.

Lara, A. H. and Wallis, J. D. (2015). The role of prefrontal cortex in working memory: A mini review. *Frontiers in Systems Neuroscience*, 9:173.

Lei, S. and Roetting, M. (2011). Influence of task combination on EEG spectrum modulation for driver workload estimation. *Human Factors*, 53(2):168–179.

Li, G. and Chung, W. Y. (2015). A context-aware EEG headset system for early detection of driver drowsiness. *Sensors*, 15:20873–20893.

Lin, C. T., Chen, S. A., Chiu, T. T., Lin, H. Z., and Ko, L. W. (2011). Spatial and temporal EEG dynamics of dual-task driving performance. *Journal of NeuroEngineering and Rehabilitation*, 8(11):1–13.

Lin, C. T., Chuang, C. H. und Kerick, S., Mullen, T., Jung, T. P., Ko, L. W., Chen, S. A., King, J. T., and McDowell, K. (2016). Mind wandering tends to occur under low perceptual demands during driving. *Sci Rep*, 17(6):21353.

Lin, C. T., Wu, R. C., Jung, T. P., Liang, S. F., and Huang, T. Y. (2005). Estimating driving performance based on EEG spectrum analysis. *EURASIP Journal on Applied Signal Processing*, 19:3165–3174.

Ling, S., Liu, T., and Carrasco, M. (2009). How spatial and feature-based attention affect the gain and tuning of population responses. *Vision Res.*, 49(10):1194–1204.

Lisman, J. (2005). The theta/gamma discrete phase code occuring during the hippocampal phase precession may be a more general brain coding scheme . *Hippocampus*, 15:913–922.

Lizarazu, M., Lallier, M., and Molinaro, N. (2019). Phase-amplitude coupling between theta and gamma oscillations adapts to speech rate. *Ann N Y Acad Sci*. doi: 10.1111/nyas.14099.

Luck, S. J. (2005). *An introduction to the event-related potential technique*. The MIT Press., Cambridge, Massachusetts.

Mai, G., Minett, J. W., and Wang, W. S. (2016). Delta, theta, beta, and gamma brain oscillations index levels of auditory sentence processing. *NeuroImage*, 133:516–528.

Mayer, A. R., Franco, A. R., Canive, J., and Harrington, D. L. (2009). The effects of stimullus modality and frequency of stimullus presentation on cross-modal distraction. *Cerebral Cortex*, 19(5):993–1007.

Mayer, A. R., Yag, Z., Yeo, R. A., Pena, A., Ling, J. M., Mannell, M. V., Stippler, M., and Mojtahed, K. (2012). A functional MRI study of multimodal selective attention following mild traumatic brain injury. *Brain Imaging and Behavior*, 6:343–354.

McGehee, D. V. (2014). Visual and cognitive distraction metrics in the age of the smart phone: A basic review. *Annals of Advances in Automotive Medicine*, 58:15–23.

Melnik, N., Mapelli, I., and Özkurt, T. E. (2017). Modulation of alpha oscillations is required for the suppression of semantic interference. *Neurobiology of Learning and Memory*, 144:11–18.

Micoulaud-Franchi, J. A., Vaillant, F., Lopez, R., Peri, P., Baillif, A., Brandejsky, L., Steffen, M. L., Boyer, L. Richieri, R., Cermolacce, M., Bioulac, S., Aramaki, M., Phillip, P., Lancon, C., and Vion/Dury, J. (2015). Sensory gating in adult with attention-deficit/hyperactivity disorder: Event-evoked potential and perceptual experience reports comparisons with schizophrenia. *Biol Psychol*, 107:16–23.

Mikutta, C., Feige, B., Maier, j. G., Hertenstein, E., Holz, J., Riemann, D., and Nissen, C. (2019). Phase-amplitude coupling of sleep slow oscillatory and spindle activity correlates with overnight memory consolidation. *J Sleep Res*, e12835. doi: 10.1111/jsr.12835.

Nandi, B., Swiatek, P., Kocsis, B., and Ding, M. (2019). Inferring the direction of rhythmic neural transmission via inter-regional phase-amplitude coupling (ir-pac). *Sci Rep*, 9(1).

Nosrati, R., Vesely, K., Schweizer, T., and Toronov, V. (2016). Event-related changes of the prefrontal cortex oxygen delivery and metabolism during driving measured by hyperspectral fnirs. *Biomedical Optics Express*, 7(4).

Oka, N., Yoshino, K., Yamamoto, K., Takahashi, H., Li, S., Sugimachi, T., Nakano, K., Suda, Y., and Kato, T. (2015). Greater activity in the frontal cortex on left curves: a vector-based fNIRS study of left and right curve driving. *PLoS One*, 10(5).

Owens, J. M., McLaughlin, S. B., and Sudweeks, J. (2011). Driver performance while text messaging using handheld and in-vehicle systems. *Accident Analysis and Prevention*, 43:939–947.

Posner, M. I., Snyder, C. R., and Davidson, B. J. (1980). Attention and the detection of signals. *J Exp Psychol*, 109(2):160–174.

Pressnitzer, D., Sayles, M., Micheyl, C., and Winter, I. M. (2008). Perceptual organization of sound begins in the auditory periphery. *Curr Biol*, 18(15):1124–1128.

Rentzsch, J., Jockers-Scherübl, M. C., Boutros, N. N., and Gallinat, J. (2008). Test-retest reliability of P50, N100 and P200 auditory sensory gating in healthy subjects. *Int J Psychophysiol*, 67(2):81–90.

Ruoff, A. (1981). *Häufigkeitswörterbuch gesprochener Sprache: gesondert nach Wortarten, alphabetisch, rückläufig alphabetisch und nach Häufigkeit geordnet*. Niemeyer.

Sabri, M., Humphries, C., Verber, M., Liebenthal, E., Binder, J. R., Mangalathu, J., and Desai, A. (2014). Neural effects of cognitive control load on auditory selective attention. *Neuropsychologia*, 61:269–279.

Sagaspe, P., Taillard, J., Akerstedt, T., Bayon, V., Espié, S., Chaumet, G., Bioulac, B., and Phillip, P. (2008). Extended driving impairs nocturnal driving performances. *PLoS one*, 3(10):1–6.

Sakihara, K., Hirata, M., Ebe, K., Kimura, K., Ryu, S. Y., Kono, Y., Muto, N., Yoshioka, M., Yoshimine, T., and Yorifuji, S. (2014). Cerebral oscillatory activity during simulated driving using MEG. *Frontiers in Human Neuroscience*, 8(975):1–9.

Sauseng, P., Klimesch, W., Doppelmayr, M., Pecherstorfer, T., Freunberger, T., and Hanslmayr, S. (2005). EEG alpha synchronization and functional coupling during top-down processing in a working memory task. *Human Brain Mapping*, 26(2):148–155.

Sauseng, P., Klimesch, W., Gruber, W. R., Hanslmayr, S., Freuenberger, R., and Doppelmayr, M. (2007). Are event-related potential components generated by phase resetting of brain oscillations? A critical discussion. *Neuroscience*, 146(4):1435–1444.

Schäfer, P. J., Corona-Strauss, F. I., Hannemann, R., Hillyard, S. A., and Strauss, D. J. (2018). Testing the limits of the stimulus reconstruction approach: Auditory attention decoding in a four-speaker free field environment. *Trends in Hearing*, 22:1–2.

Schweizer, T. A., Kan, K., Hung, Y., Tam, F., Naglie, G., and Graham, S. J. (2013). Brain activity during driving with distraction: an immersive fmri study. *Frontiers in Human Neuroscience*, 7(53):1–11.

Solis-Marcos, I., Galvao-Carmona, A., and Kircher, K. (2017). Reduced attention allocation during short periods of partially automated driving: An event-related potentials study. *Front Hum Neurosci*, 11:537.

Stein, T. and Peelen, M. V. (2015). Content-specific expectations enhance stimulus detectability by increasing perceptual sensitivity. *J Exp Psychol Gen.*, 144(6):1089–1104.

Tallon-Baudry, C., Bertrand, O., Delpuech, C., and Pernier, J. (1997). Oscillatory gamma-band (30-70 Hz) activity induced by a visual search task in humans. *The Journal of Neuroscience*, 17(2):722–734.

Tijerina, L., Johnston, S., Parmer, E., and Winterbottom, M. D. (2000). Driver distraction with wireless telecommunications and route guidance systems. Technical Report DOT HS 809-0692, National Highway Traffic Safety Administration, U. S. Department of Transportation.

Tort, A. B. L., Komorowski, R., Eichenbaum, H., and Kopell, N. (2010). Measuring phase-amplitude coupling between neuronal oscillations of different frequencies. *J. Neurophysiol*, 104:1195–1210.

Tzvi, E., Bauhaus, L. J., Kessler, T. U., Liebrand, M., Wöstmann, M., and Krämer, U. M. (2018). Alpha-gamma phase amplitude coupling subserves information transfer during perceptual sequence learning. *Neurobiology of Learning and Memory*, 149(1):107–117.

Uhlhaas, P. J., Roux, F., Rodriguez, E., Rotarska-Jagiela, A., and Singer, W. (2009). Neural synchrony and the development of cortical networks. *Trends in Cognitive Sciences*, 14(2):72–80.

van den Berg, B., Appelbaum, L. G., Clark, K., Lorist, M. M., and Woldorff, M. G. (2016). Visual search performance is predicted by both prestimulus and poststimulus electrical brain activity. *Sci Rep*, 6(37718; doi: 10.1038/srep37718).

van Diepen, R. M. and Mazaheri, A. (2017). Cross-sensory modulation of alpha oscillatory activity: suppression, idling, and default resource allocation. *European Journal of Neuroscience*, 45:1431–1438.

Wang, W., Shivakumar, V., Lee, T., and Grafton, S. T. (2016). Coupling between Theta Oscillations and Cognitive Control Network during Cross-Modal Visual and Auditory Attention: Supramodal vs Modality-Specific Mechanism. *PLOS One*, 11(7, doi:10.1371/journal.pone.0158465):e0158465.

Wascher, E., Getzmann, S., and Karthaus, M. (2016). Driver state examination - treading new paths. *Accident Analysis and Prevention*, 91:157–165.

Weise, A., Hartmann, T., Schröger, E., Weisz, N., and Ruhnau, P. (2016). Cross-modal distractors modulate oscillatory alpha power: the neural basis of impaired task perfomance. *Psychophysiology*, 53:1651–1659.

Wetzel, N., Schröger, E., and Widmann, A. (2013). The dissociation between the P3a event-related potential and behavioral distraction. *Psychophysiology*, 50(9):920–930.

Wolfe, J. M. (2010). Visual search. *Curr Bio*, 20(8):R346–R349.

Wolfe, J. M. and Horowitz, T. S. (2004). What attributes guide the deployment of visual attention and how do they do it? *Nature Reviews Neuroscience*, 5:495–501.

Wöstmann, M., Lim, S., and Obleser, J. (2017). The human neural alpha response to speech is a proxy of attentional control. *Cerebral Cortex*, 27(6):3307–3317.

Yan, L., Wang, Y., Ding, C., Liu, M., Yan, F., and Guo, K. (2019). Correlation among behavior, personality, and electroencephalography revealed by a simulated driving experiment. *Front Psychol*, 10:1524.

Yoshino, K., Oka, N., Yamamoto, K., Takahashi, H., and Kato, T. (2013). Functional brain imaging using near-infrared spectroscopy during actual driving on an expressway. *Frontiers in Human Neuroscience*, 7(882):1–16.

Young, K. and Regan, M. (2007). Driver distraction: A review of the literature. In Faulks, I. J., Regan, M., Stevenson, M., Brown, J., Porter, A., and Irwin, J., editors, *Distracted driving*, pages 379–405. Australasian College of Road Safety, Sydney.

Publications by the author

Publications as a first author (in reverse chronological order, newest first), relevant to the thesis:

- **Gonzalez Trejo E**, Mögele H, Pfleger N, Hannemann R, Strauss DJ (2019) "Electroencephalographic Phase-Amplitude Coupling in Simulated Driving with Varying Modality-Specific Attentional Demand". IEEE Transactions on Human-Machine Systems, vol. 49, issue 6, pp. 589-598.
- **Gonzalez Trejo E**, Schäfer PJ and Strauss DJ (2021) "Auditory Stimulus Reconstruction in a Simulated Driving Environment - Decoding of Auditory Attention in a Situation with Varying Modality-Specific Attentional Demand" , IEEE Transactions on Human-Machine Systems, *in preparation*.

Publications as a first author (in reverse chronological order, newest first), relevant to the thesis:

- **Gonzalez Trejo E**, Kohl M, Steinbach A, Mögele H, Pfleger N, Strauss DJ (2015) "Correlation Between Cortical Inhibition and Auditory Stream Segregation in a Driving Environment". 7th Annual IEEE EMBS Conference on Neural Engineering, Montpellier, France.
- **Gonzalez Trejo E**, Herrmann D, Kohl M, Corona-Strauss FI, Strauss DJ (2013) "Paired chirp evoked cortical inhibition and its behavioral correlates in a speech intelligibility task", Int. IEEE/EMBS Conf. Neural Eng. NER.

Publications as a coauthor (in reverse chronological order, newest first), relevant to the thesis:

- Strauss DJ, Damian A, **Gonzalez Trejo E**, Hannemann R, Mögele H, Corona-Strauss FI (2016) "Neural Correlates of Listening Effort in a Multimodal Interactive Driving Environment" in HEAL-Hearing Across the Lifespan, 2016

Publications as a coauthor (in reverse chronological order, newest first), not directly relevant to the thesis:

- Schubert JK, **Gonzalez Trejo E**, Retz W, Rösler M, Corona-Strauss FI, Steidl G, Teuber T, Strauss DJ (2014) "Dysfunctional cortical inhibition in adult ADHD: neural correlates in auditory event-related potentials" J. Neurosci. Methods, vol. 235, pp. 181-188, Sep.

- Retz W, **Gonzalez Trejo E**, Römer KD, Philipp-Wiegmann F, Reinert P, Low YF, Boureghda S, Rösler M, Strauss DJ (2012) "Assessment of post-excitatory long-interval cortical inhibition in adult attention-deficit/hyperactivity disorder" Eur. Arch. Psychiatry Clin. Neurosci., vol. 262, no. 6, pp. 507-517, Feb.

Acknowledgements

Thanks to Prof. Dr. Dr. Daniel J. Strauss for the opportunity to pursue my scientific interests in the field of neurosciences. In the time I spent at the SNN-Unit, I was able to work in a variety of state of the art projects both in the fields of neurophysiopathologies (ADHD), fundamental neuroscience (modeling of neural fields) and finally the main theme of my thesis, neuroergonomy and human-machine interfaces. Thanks to the department of Forensic Neuroscience in the Uniklinik Homburg, especially to Prof. Retz and Prof. Rösler, who allowed me to develop the ground work necessary for the evaluation of attentional tasks in auditory evoked potentials. Likewise, to the industry partners who made possible the collaboration between SNN Unit and Audi/Semvox for working with human-machine interfaces, Dr. Hannes Mögele and Dr. Norbert Pfleger. Also to Dr. Hannemann for the review of the paradigm designed for the main work of the thesis.

Thanks to Dr. Corinna Bernarding, Dr. Farah I. Corona-Strauss, Dr. Lars Haab and (alumni) Dr. Novaf Özgün and Dr. Michael Busse for their unconditional support since the first day I started working there. Without their feedback, corrections and motivation this thesis would not have been possible. Likewise a big thank you to my colleagues during the master study and promotion, Ing. Alejandro E. Romero Santiago, Kristof Schubert, Philipp Flotho, Manuel Kohl, Patrick Schäfer, Erik Schebsdat, Alexander Steinbach, and the alumni David Herrmann, Kevin Kern, Vladislav Royter, Dr. Yin Fen Low and Dr. Mathias Vukelic. To all the students (and colleagues) who offered their time as tests subjects, thanks a lot.

To my professors in Mexico City in the Universidad Iberoamericana: Dr. Luis Clemente Jimenez Botello, Jorge Andres Martinez Alarcon, M. Sc. and Jose Luis Urrusti Alonso, M. Sc. and Felix Leon De Alba, M. Sc., for teaching me the principles of hard work, dedication and most of all the love for biomedical engineering in all its aspects, thank you.

Last but not least, to my wife and her unconditional support before and during doctoral thesis. Without the support I had at home, none of this would have been possible.